LASER INTERFEROMETER GRAVITATIONAL WAVE OBSERVATORY

LIGO Laboratory / LIGO Scientific Collaboration

LIGO-T080073-01-D *ADVANCED LIGO* 03/28/08

ETM Reaction Mass Optical Irregularity Effect on the ETM Output Spot Size

Michael Smith

Distribution of this document:
LIGO Science Collaboration

This is an internal working note
of the LIGO Project.

California Institute of Technology
LIGO Project – MS 18-34
1200 E. California Blvd.
Pasadena, CA 91125
Phone (626) 395-2129
Fax (626) 304-9834
E-mail: info@ligo.caltech.edu

Massachusetts Institute of Technology
LIGO Project – NW22-295
185 Albany St
Cambridge, MA 02139
Phone (617) 253-4824
Fax (617) 253-7014
E-mail: info@ligo.mit.edu

LIGO Hanford Observatory
P.O. Box 1970
Mail Stop S9-02
Richland WA 99352
Phone 509-372-8106
Fax 509-372-8137

LIGO Livingston Observatory
P.O. Box 940
Livingston, LA 70754
Phone 225-686-3100
Fax 225-686-7189

http://www.ligo.caltech.edu/

Table of Contents

Appendices

Error! No table of figures entries found.

Table of Tables

Table of Figures

Abstract

This document describes quantitatively the effect of optical distortions in the ETM Reaction Mass on the output spot shape and position at the quad photodiode of the ETM output beam monitor. The results were calculated using Zemax Optical Design Program; physical optics propagation program.

Based on these results, we conclude that the ADLIGO ETM reaction mass can be specified to have less than 2.5 waves of astigmatic and comatic phase irregularity, as well as high order distortions in transmission over the central 160 mm diameter clear aperture of the optic.

1 Introduction

1.1 Purpose

The purpose of this document is to describe quantitatively the effect of optical distortions in transmission through the ETM Reaction Mass on the output spot shape and location at the quad photodiode of the ETM output beam monitor.

1.2 Scope

This analysis is limited to simulated astigmatic and comatic optical distortions placed on the output face of the ETM reaction mass, as specified by the appropriate Zernike polynomials.

The analysis was done using Zemax Optical Design Program; physical optics propagation program.

The modeled sequential optical system consisted of the ETM reaction mass, the Initial LIGO ETM Telescope, a commercial 125mm focal length lens, with the QPD placed nominally at the focal plane of the lens.

1.3 Definitions

Astigmatism is the peak amplitude of the phase distortion across the surface of the optic specified in optical wavelengths, described as a function of the normalized radius and the azimuthal angle and specified analytically by the 5^{th} and 6^{th} Zernike polynomials with n=2, m=2 (see Zemax Optical Design Program, Zemax Development Corp, Zernike Standard Polynomials; or Principles of Optics, Born & Wolf, Pergamon Press).

Coma is the peak amplitude of the phase distortion across the surface of the optic specified in optical wavelengths, described as a function of the normalized radius and the azimuthal angle and specified analytically by the 7^{th} and 8^{th} Zernike polynomials with n=3, m=1 (see Zemax Optical Design Program, Zemax Development Corp; Zernike Standard Polynomials, or Principles of Optics, Born & Wolf, Pergamon Press).

1.4 Acronyms

COS	Core Optics Support
ETM	End Test Mass
IFO	Interferometer
QPD	quadrant photodiode
ADLIGO	Advanced LIGO

1.5 Applicable Documents

1.5.1 LIGO Documents

T980104-00 COS Final Design

1.5.2 Non-LIGO Documents

Principles of Optics, Born & Wolf, Pergamon Press

Zemax Optical Design Program, Zemax Development Corp;

2 Optical Layout

The optical layout that is modeled with Zemax is shown in Figure 1.

A Zernike phase function is applied on the back face of the reaction mass. The radial dimension is normalized to the maximum clear aperture diameter of 160 mm.

A 160 mm diameter circular aperture is placed in front of the entrance aperture of the Initial LIGO ETM telescope.

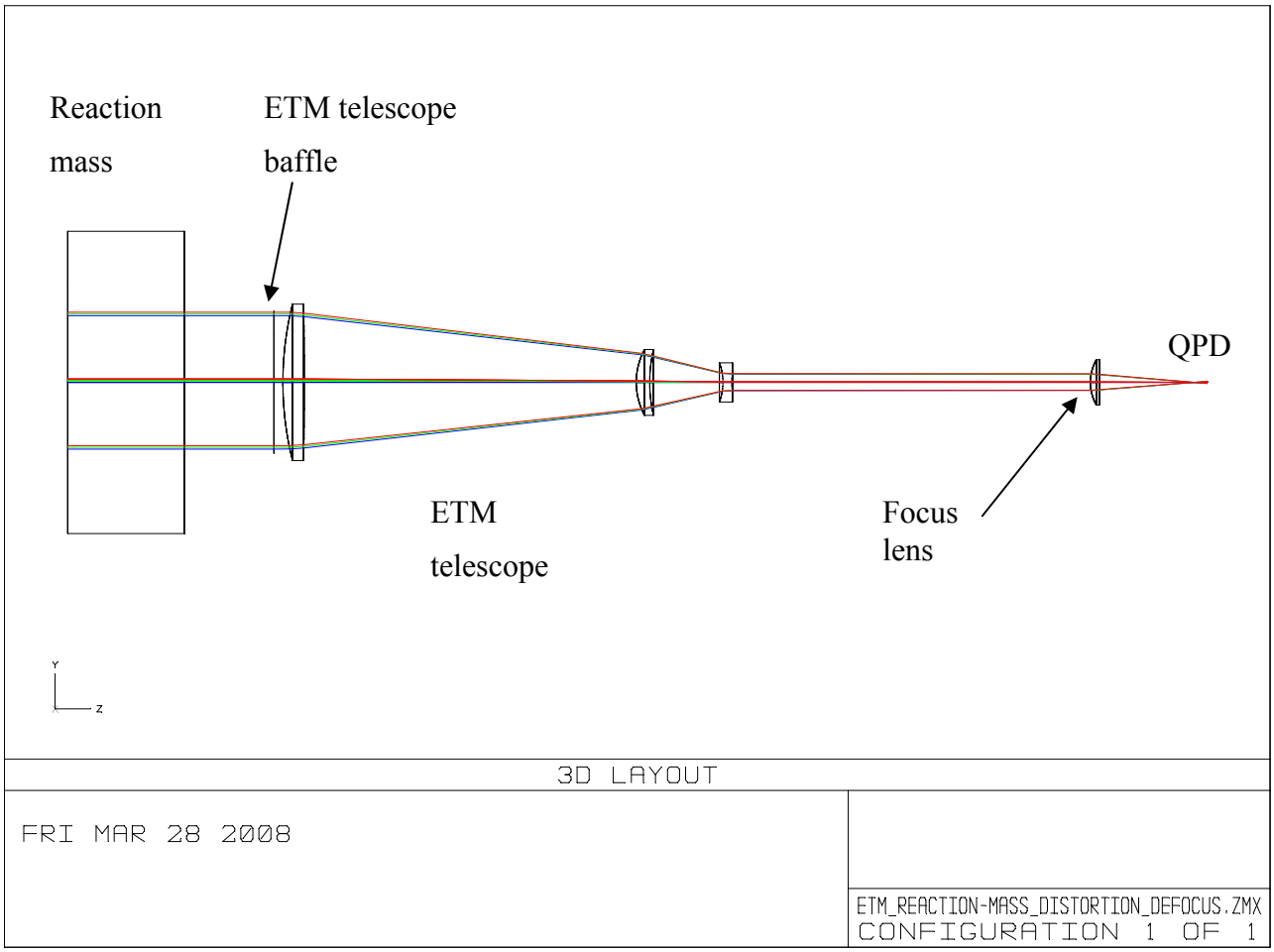

Figure 1: Optical Layout for Analyzing the Effect of Reaction Mass Optical Distortions on the ETM Output Focused Spot Shape

The Initial LIGO ETM telescope is a three-element refractive afocal telescope with a beam reduction ratio of 8:1 (Ref: COS Final Design).

A 1064 nm Gaussian beam with a 11.5 mm waist located 2E6 mm to the left in the figure is incident on the ETM reaction mass.

The output beam from the ETM telescope is de-focused onto the QPD with a CVI PLCX-50.8-51.5 plano convex focus lens, with a focal length of approximately 100 mm. The defocus distance was chosen to produce a spot diameter of approximately 1.0 mm at the QPD.

3 Results

The calculated X and Y spot cross section profiles and the centroid coordinates of the spot at the QPD are shown in the following figures.

Spot profiles and spot centroid coordinates were calculated with the IFO beam on-axis and at two off-axis field angles— 5.7E-5 deg and 1.1E-4 deg, which correspond respectively to 2 mm and 4 mm displacements of the IFO beam from the center the ETM.

3.1 Spot Shape with No Optical Distortion of Reaction Mass

3.1.1.1 On-axis

3.1.1.1.1 X Cross Section

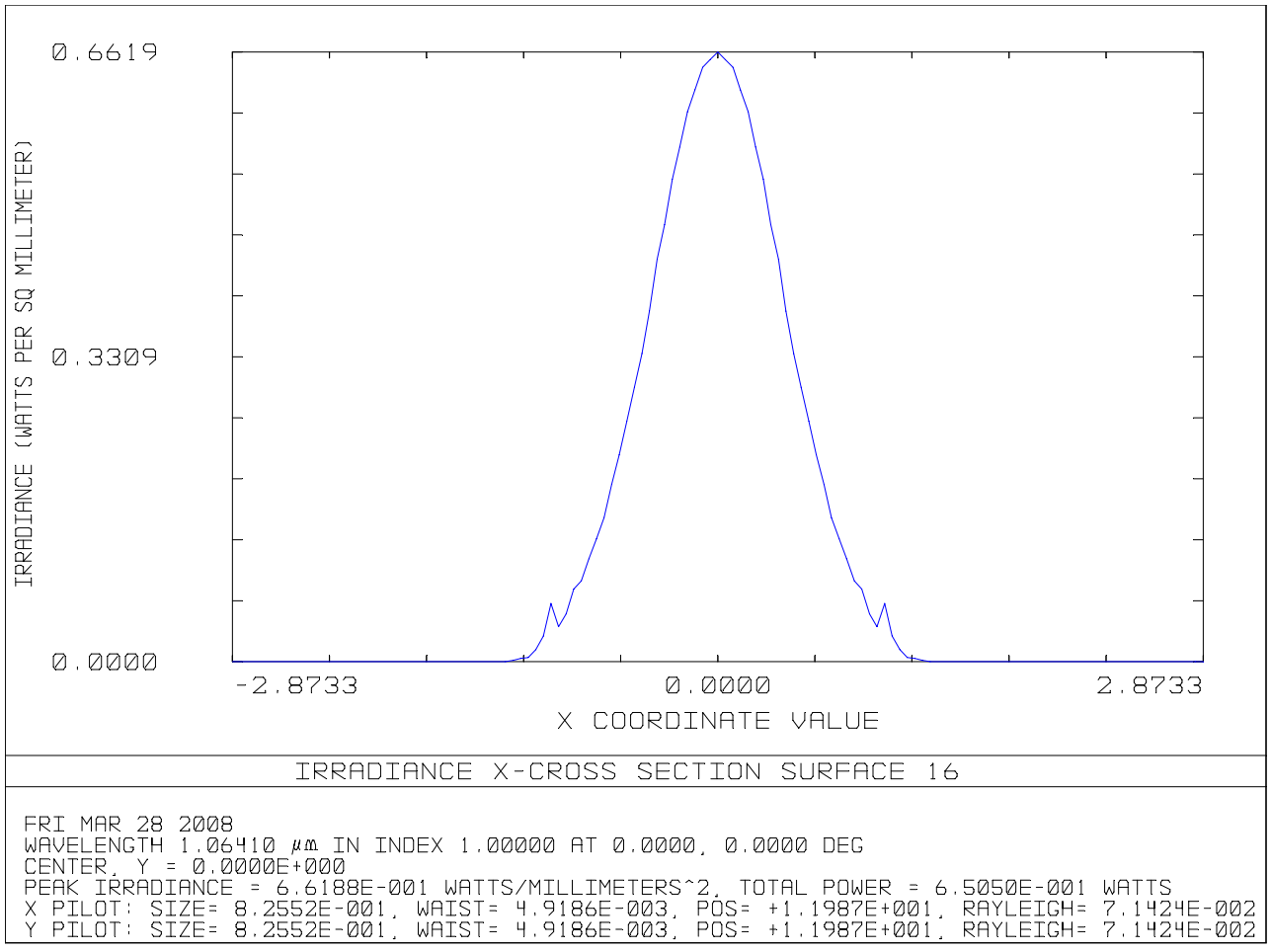

Figure 2: On-axis spot, X Cross Section, No Distortion

3.1.1.1.2 Y Cross Section

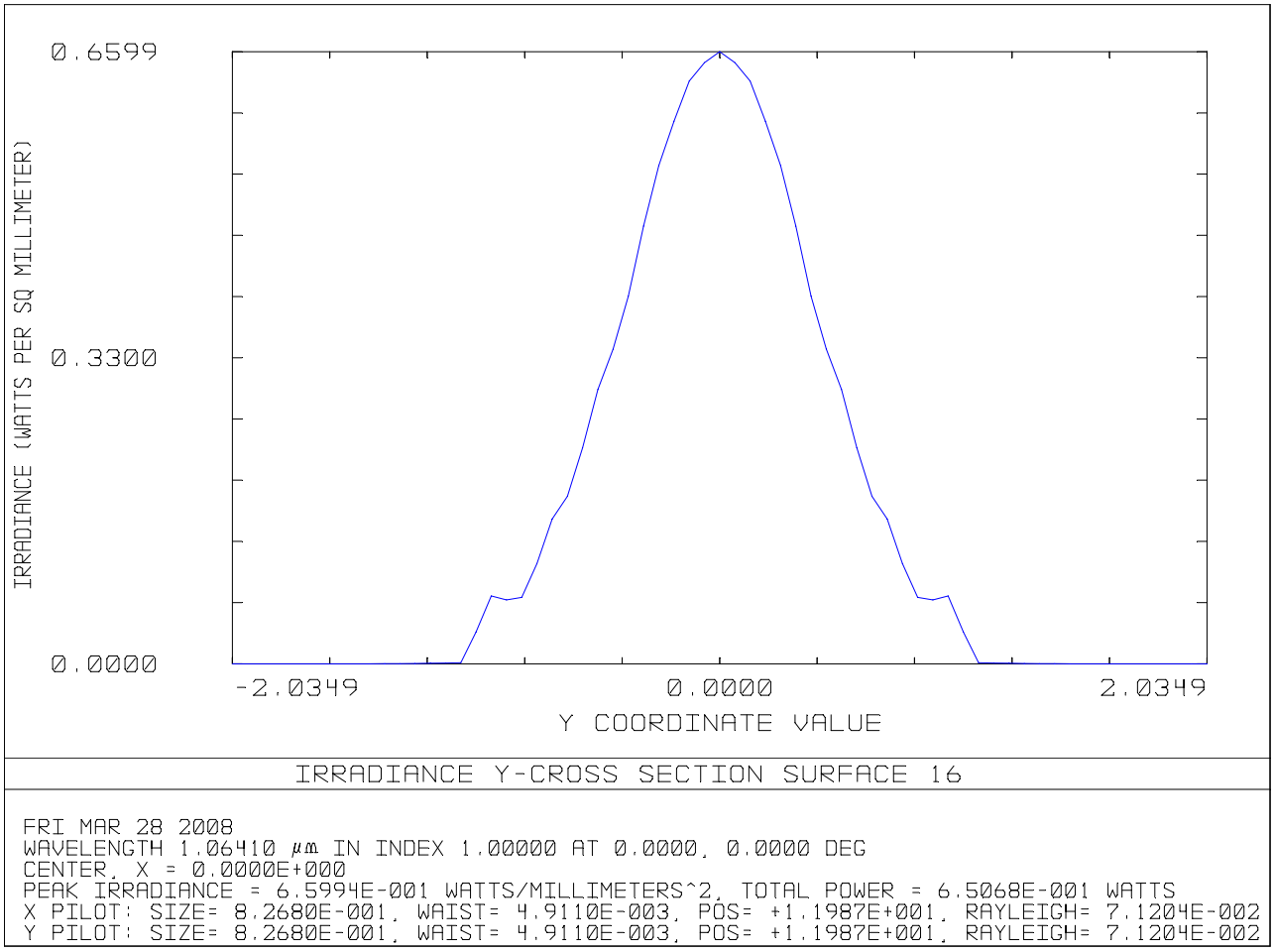

Figure 3: On-axis spot, Y Cross Section, No Distortion

3.1.1.2 Off-axis, 4 mm

3.1.1.2.1 X Cross Section

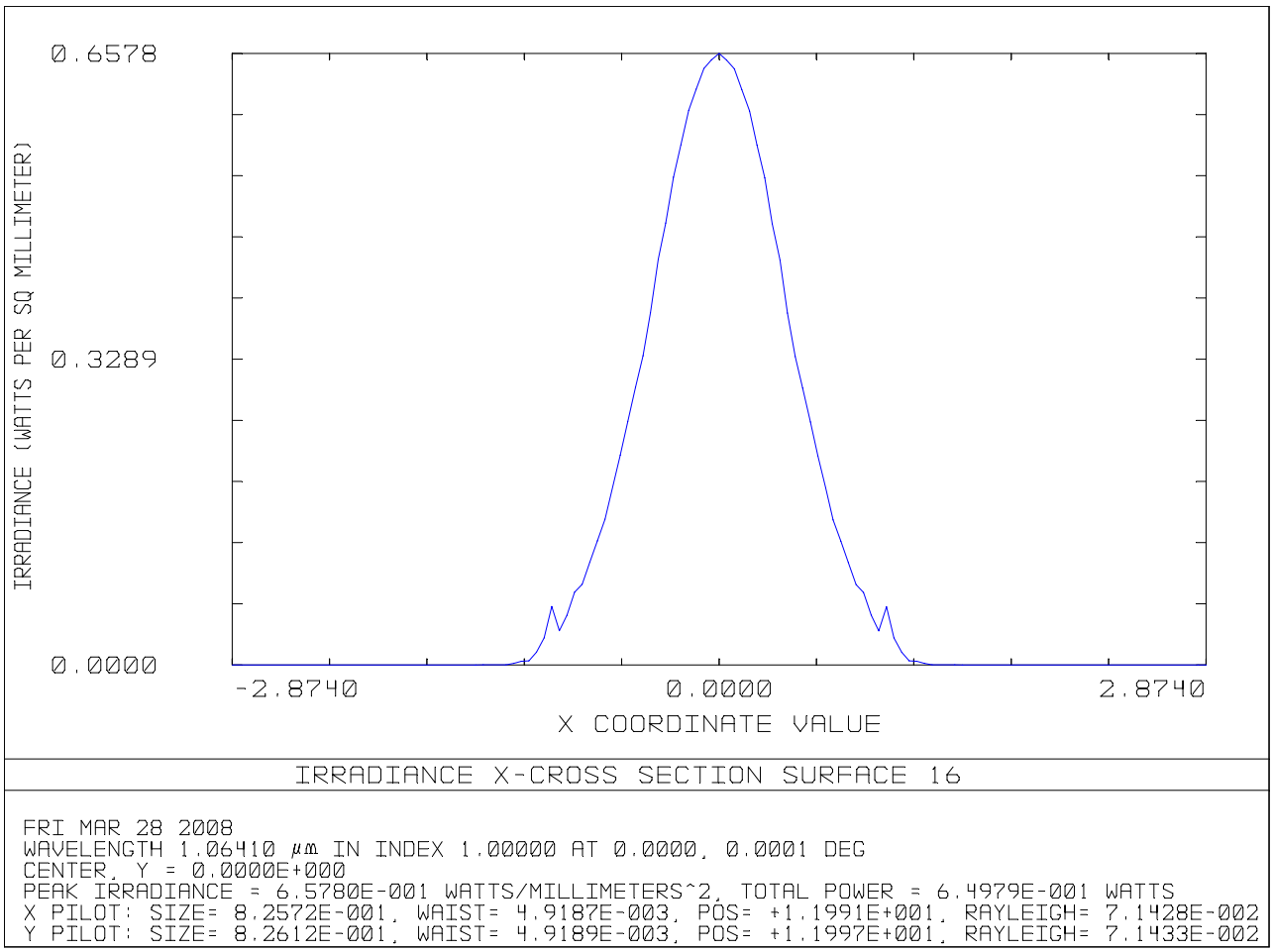

Figure 4: Off-axis 4 mm spot, X Cross Section, No Distortion

3.1.1.2.2 Y Cross Section

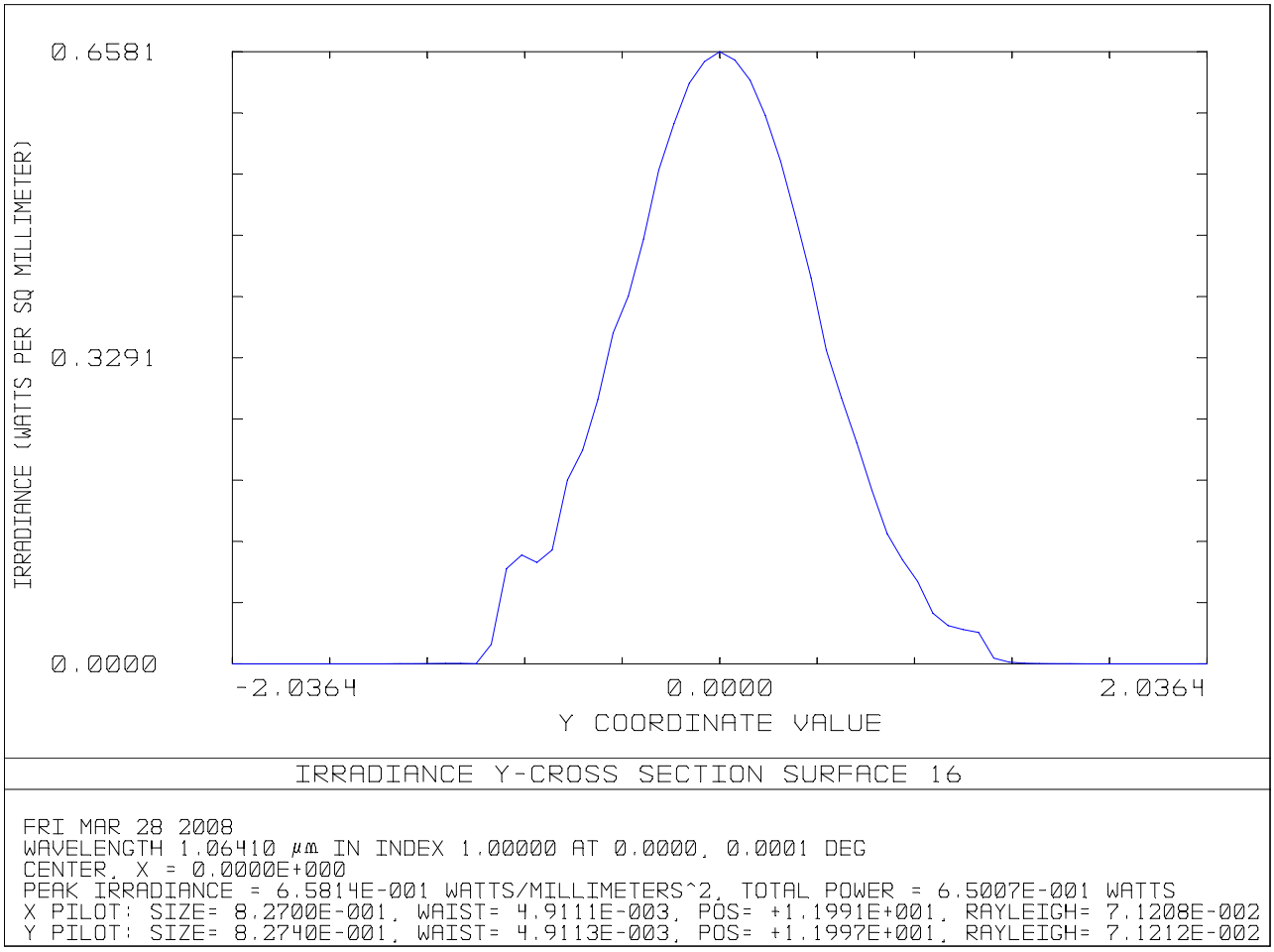

Figure 5: Off-axis 4 mm spot, Y Cross Section, No Distortion

3.2 Effects of Astigmatism on the Output Spot Shape

The Zernike polynomial for astigmatism is the following (see Zemax Optical Design Program, Zemax Development Corp; Zernike Standard Polynomials):

$$\sqrt{6}\cdot\left(\rho^2\cdot\cos(2\phi)\right)$$

Where ρ is the radial dimension normalized to the maximum radius, 80 mm, of the optical surface in the X-Y plane, and φ is the azimuthal angle measured counter clockwise from the local +X axis.

3.2.1 1.25 Waves of Astigmatic Phase Distortion

Note in the following figures that the distortion of the spot shape does not vary significantly for the three field positions.

3.2.1.1 On-axis

3.2.1.1.1 X Cross Section

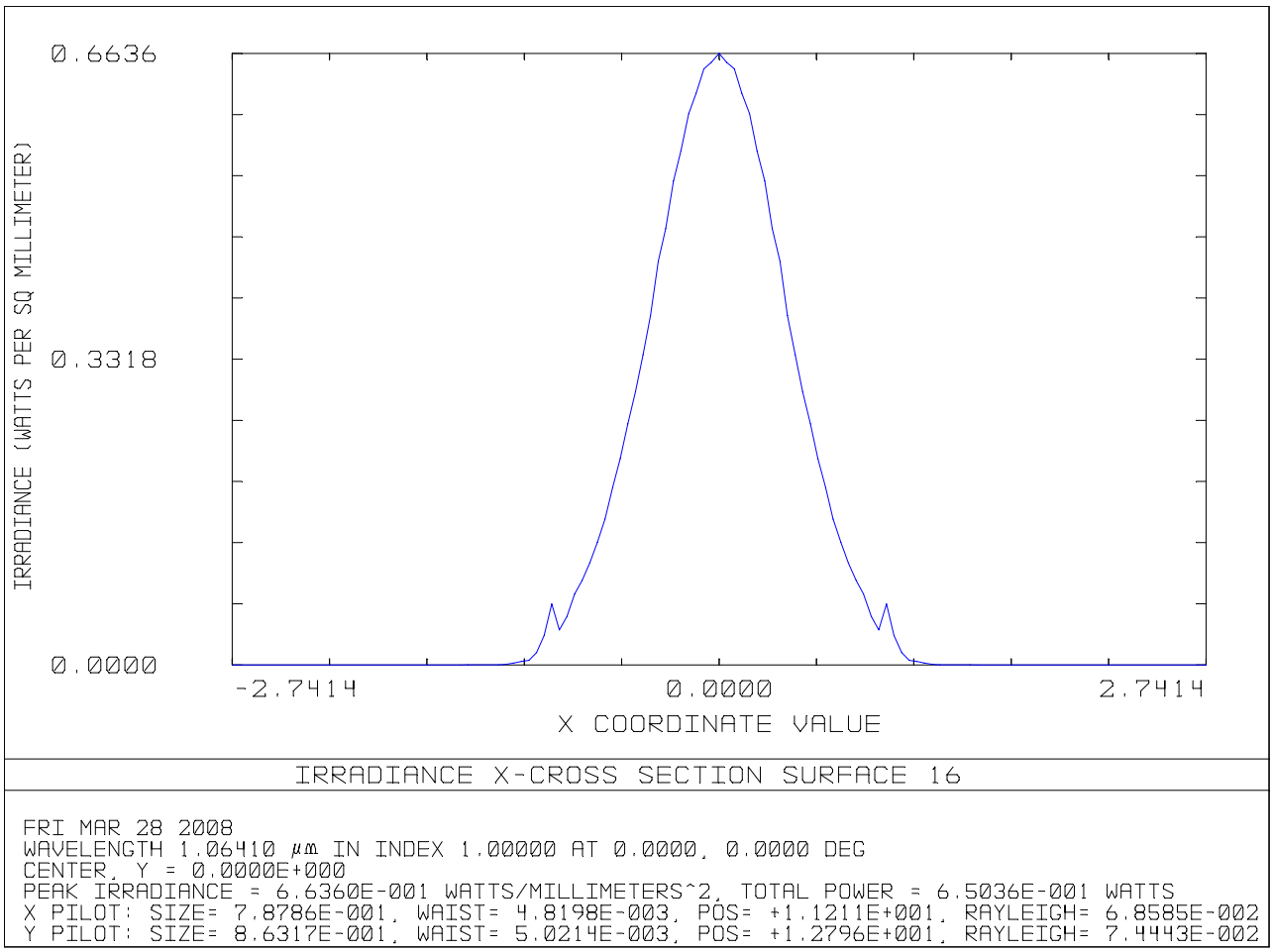

Figure 6: On-axis spot, X Cross Section, 1.25 Waves Astigmatic Distortion

3.2.1.1.2 Y Cross Section

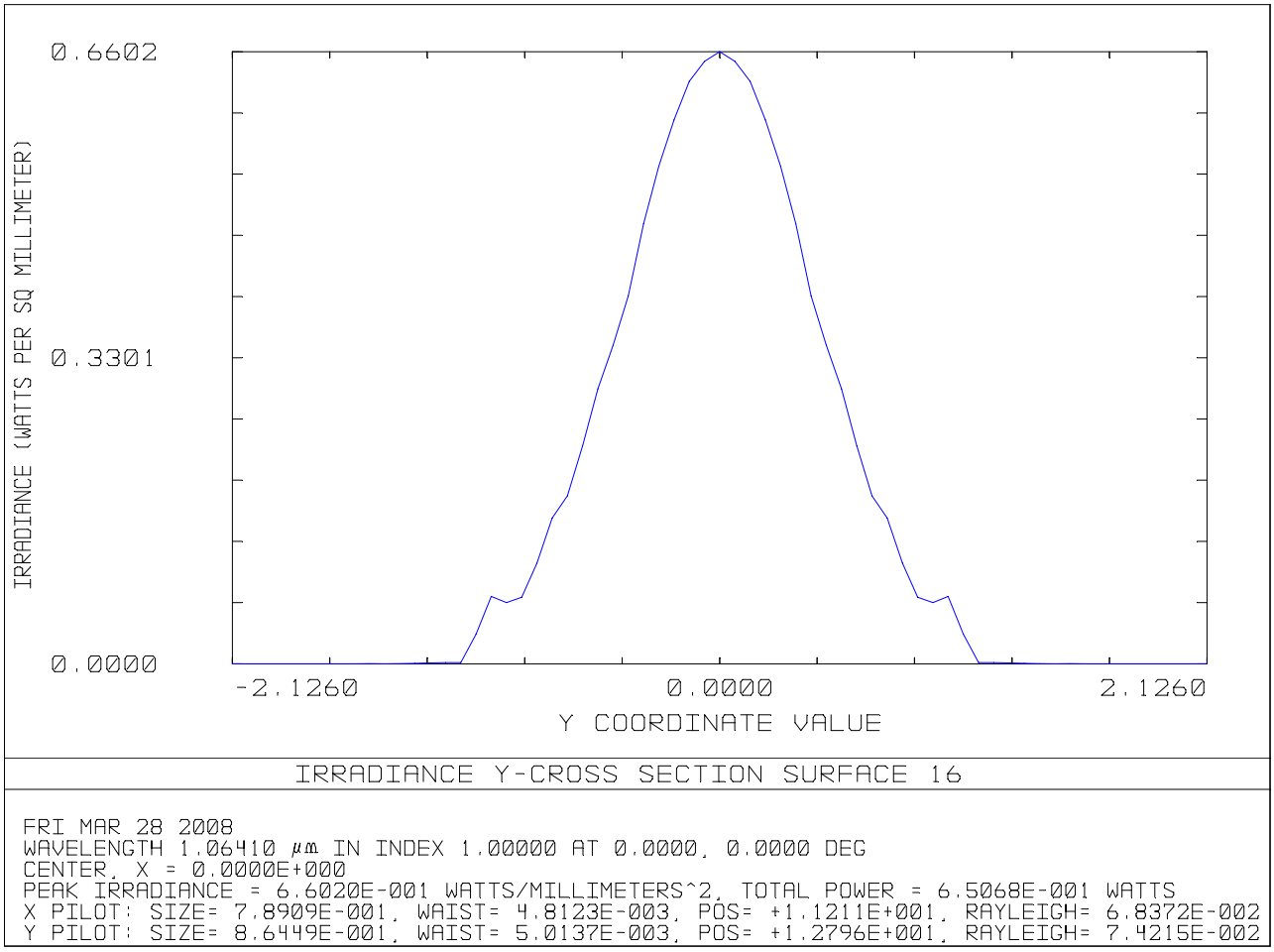

Figure 7: On-axis spot, Y Cross Section, 1.25 Waves Astigmatic Distortion

3.2.1.2 Off-axis, 4 mm

3.2.1.2.1 X Cross Section

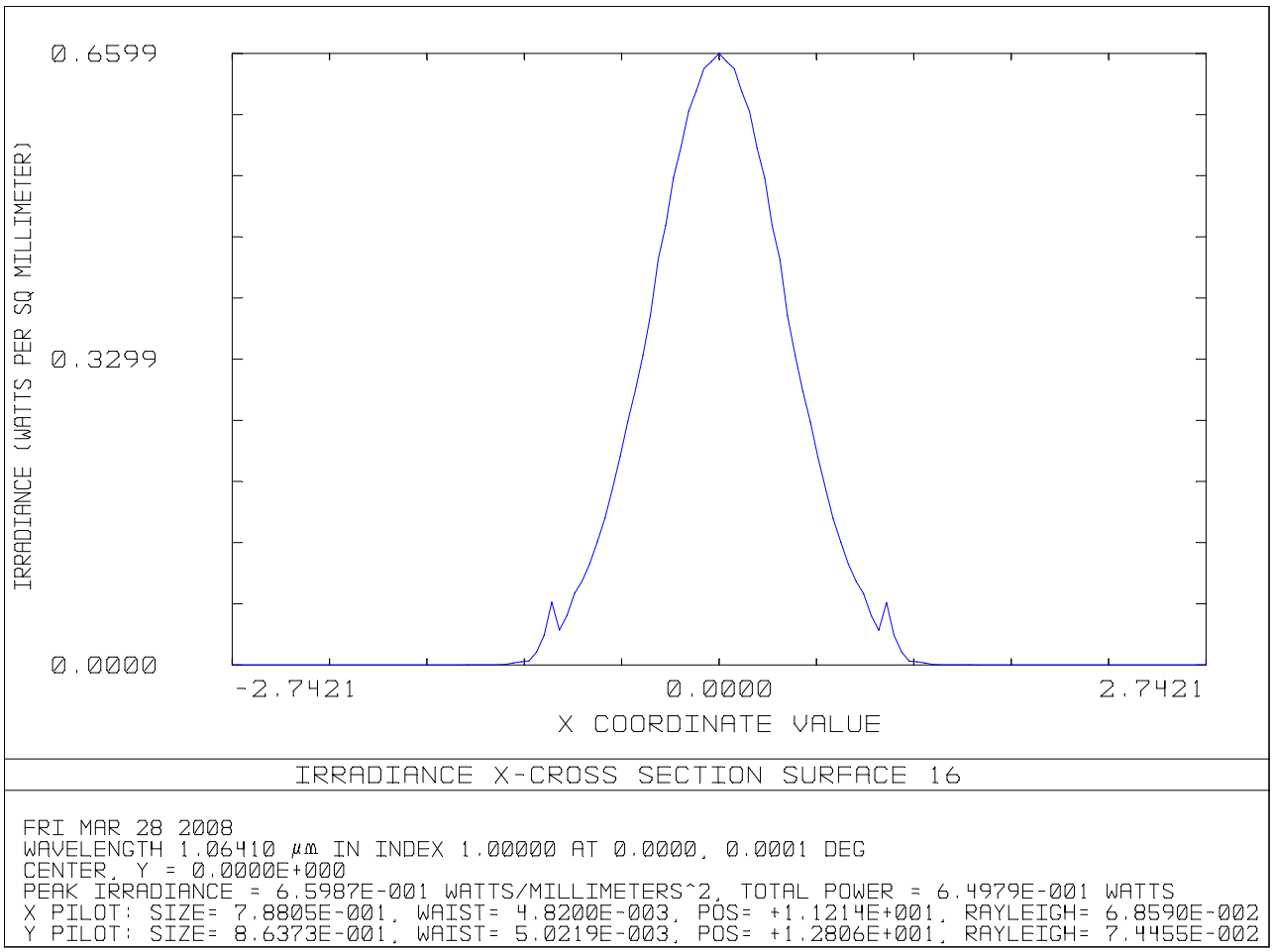

Figure 8: Off-axis 4 mm spot, X Cross Section, 1.25 Waves Astigmatic Distortion

3.2.1.2.2 Y Cross Section

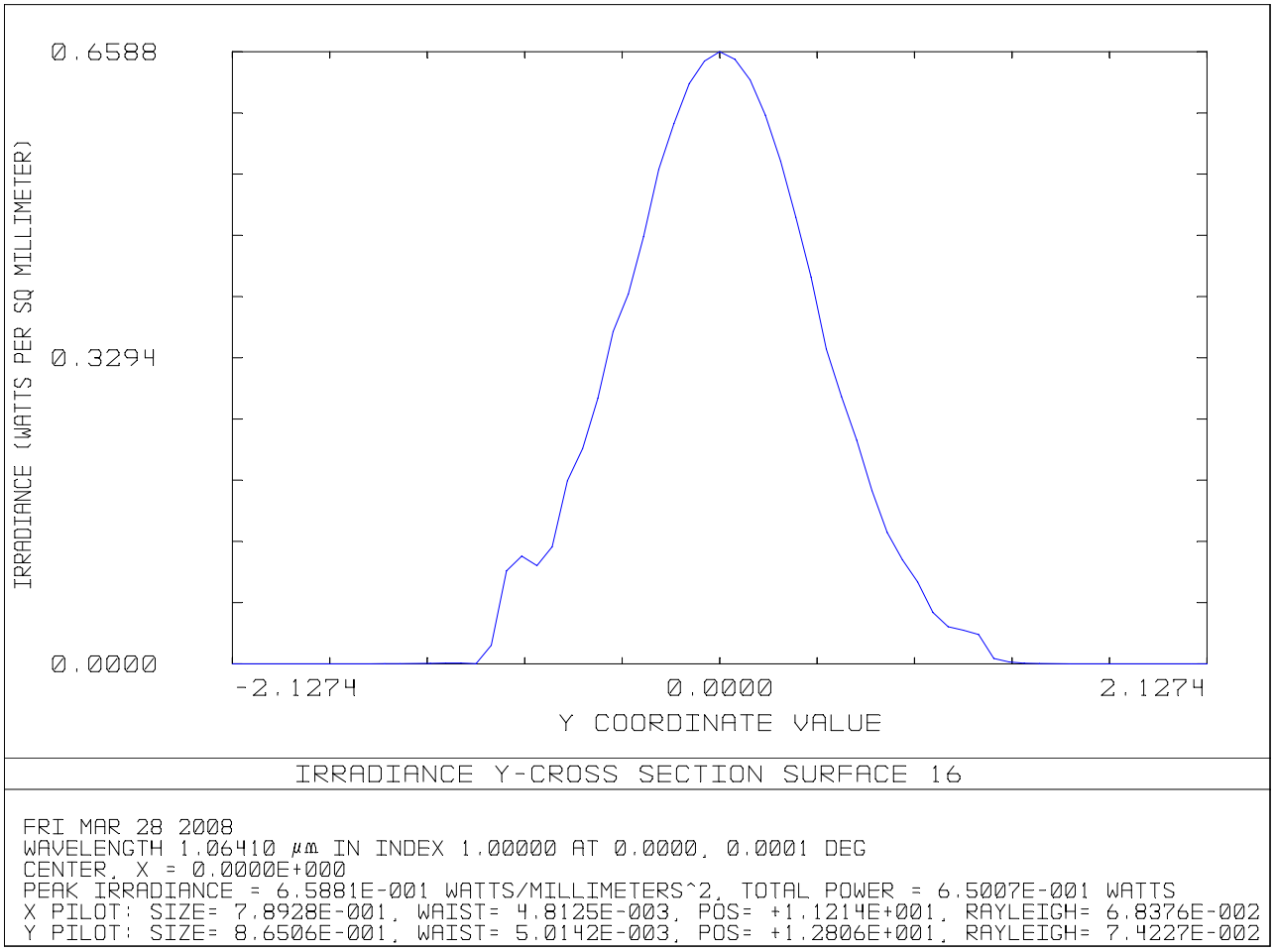

Figure 9: Off-axis 4 mm spot, Y Cross Section, 1.25 Waves Astigmatic Distortion

3.2.2 2.5 Waves of Astigmatic Phase Distortion

Note in the following figures that the distortion of the spot shape is identical for the on-axis and the 4 mm field positions.

3.2.2.1 On-axis

3.2.2.1.1 X Cross Section

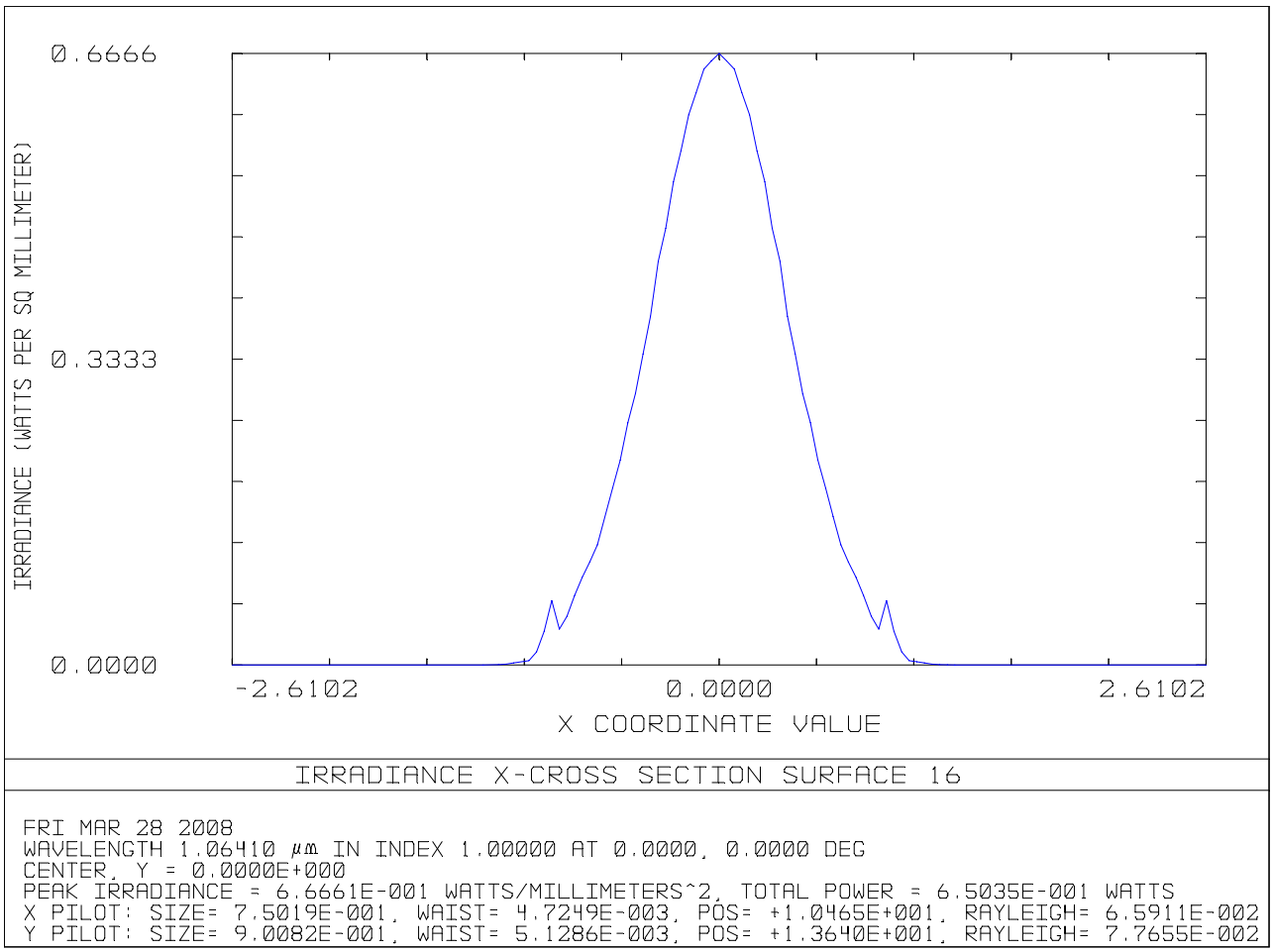

Figure 10: On-axis spot, X Cross Section, 2.5 Waves Astigmatic Distortion

3.2.2.1.2 Y Cross Section

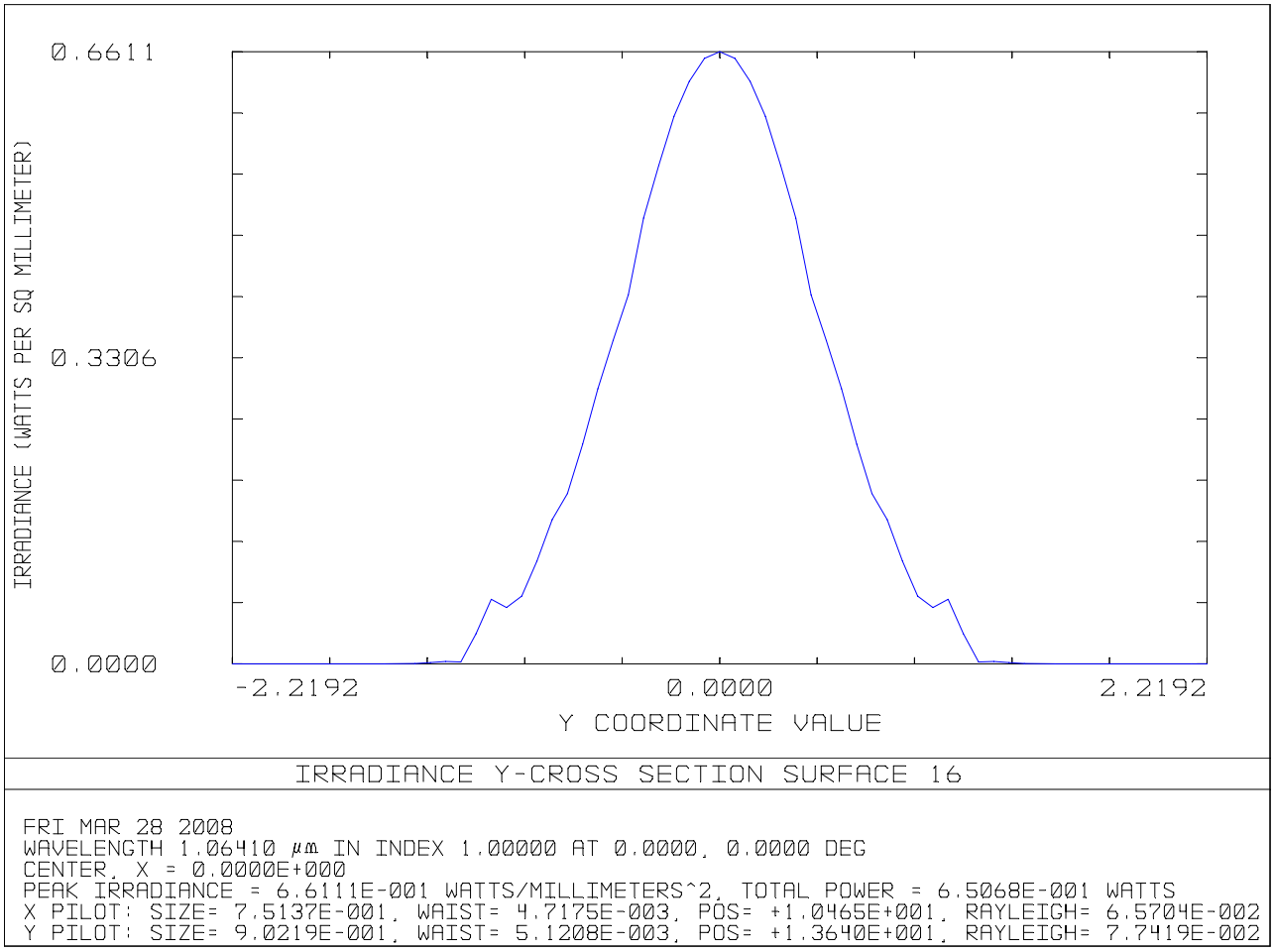

Figure 11: On-axis spot, Y Cross Section, 2.5 Waves Astigmatic Distortion

3.2.2.2 Off-axis, 4 mm

3.2.2.2.1 X Cross Section

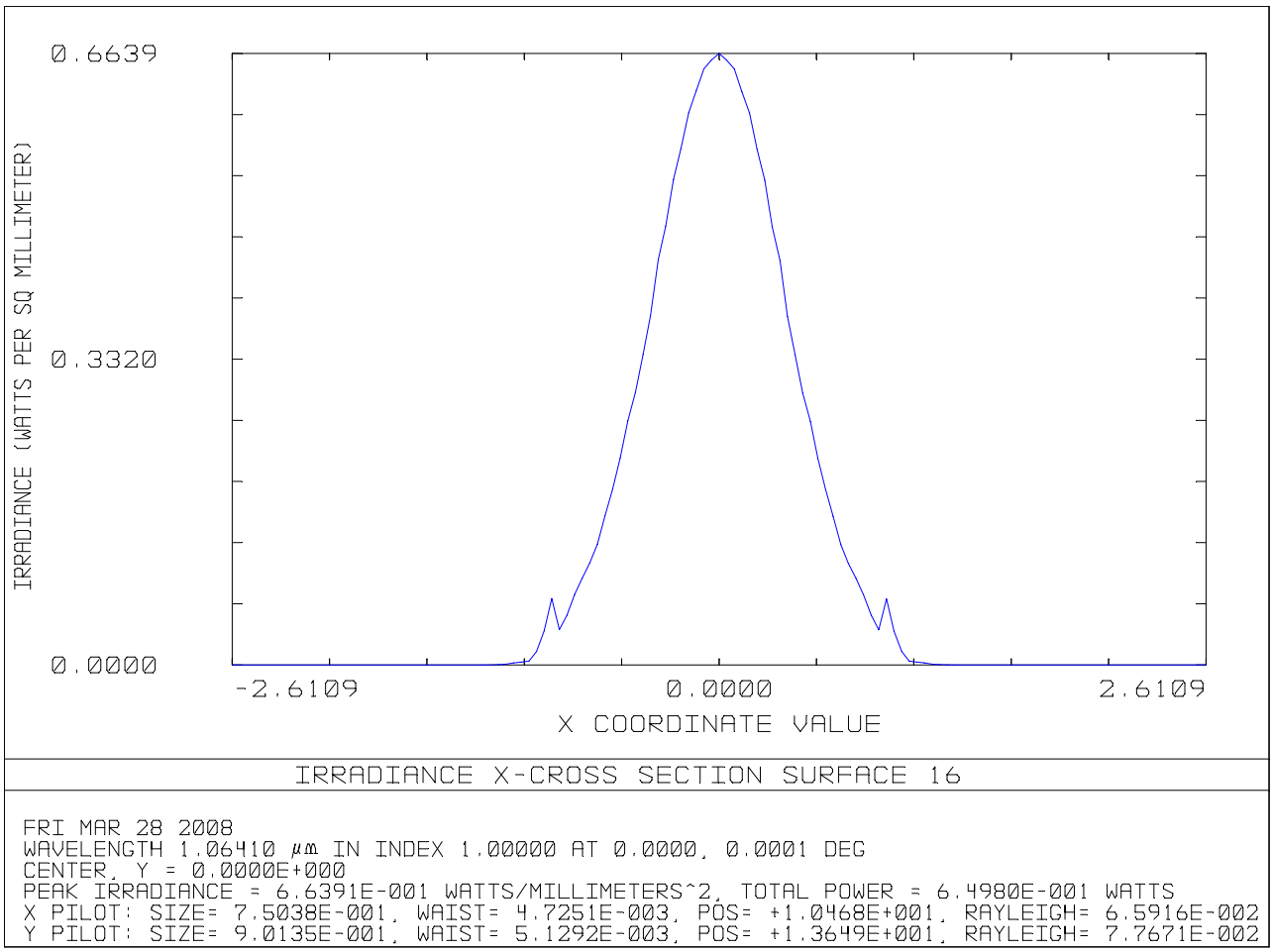

Figure 12: Off-axis 4 mm spot, X Cross Section, 2.5 Waves Astigmatic Distortion

3.2.2.2.2 Y Cross Section

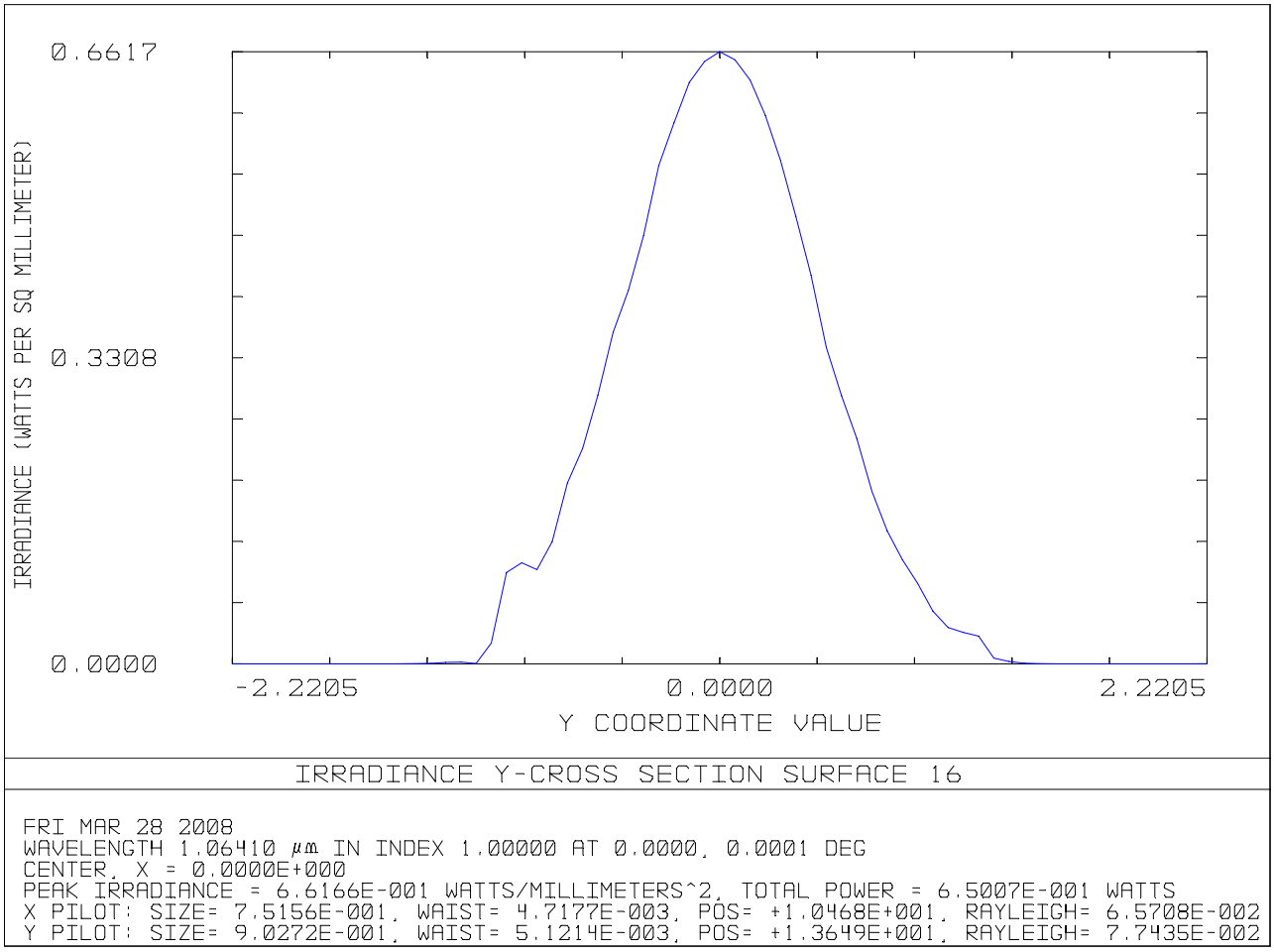

Figure 13: Off-axis 4 mm spot, Y Cross Section, 2.5 Waves Astigmatic Distortion

3.3 Effects of Coma on the Output Spot Shape

The Zernike polynomial for coma is the following (see Zemax Optical Design Program, Zemax Development Corp; Zernike Standard Polynomials):

$$\sqrt{8}\cdot\left(3\cdot\rho^3-2\cdot\rho\right)\cdot\cos(\phi)$$

3.3.1 0.6 Waves of Comatic Phase Distortion

Note in the following figures that the distortion of the spot shape does not vary significantly for the three field positions.

3.3.1.1 On-axis

3.3.1.1.1 X Cross Section

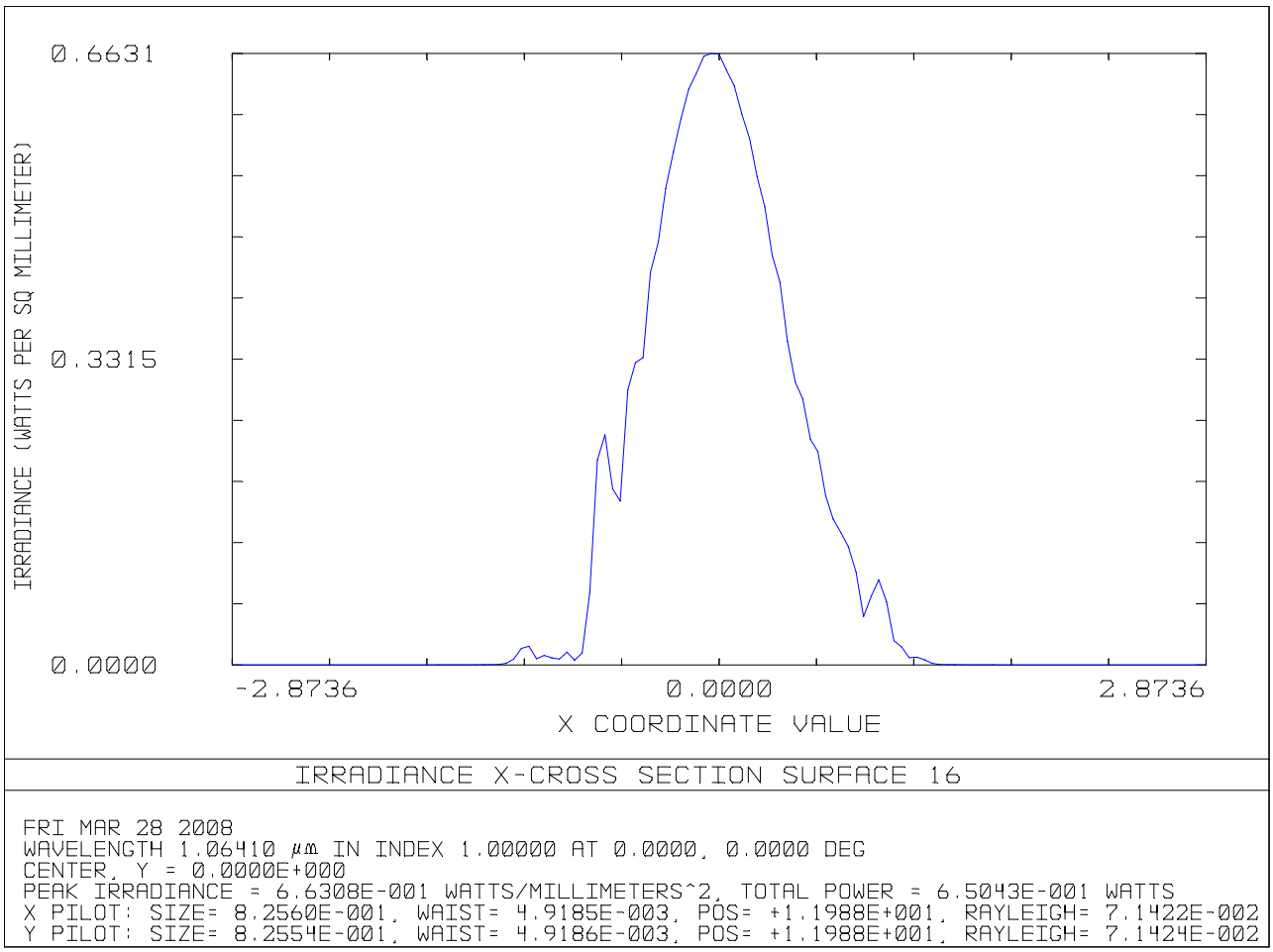

Figure 14: On-axis spot, X Cross Section, 0.6 Waves Comatic Distortion

3.3.1.1.2 Y Cross Section

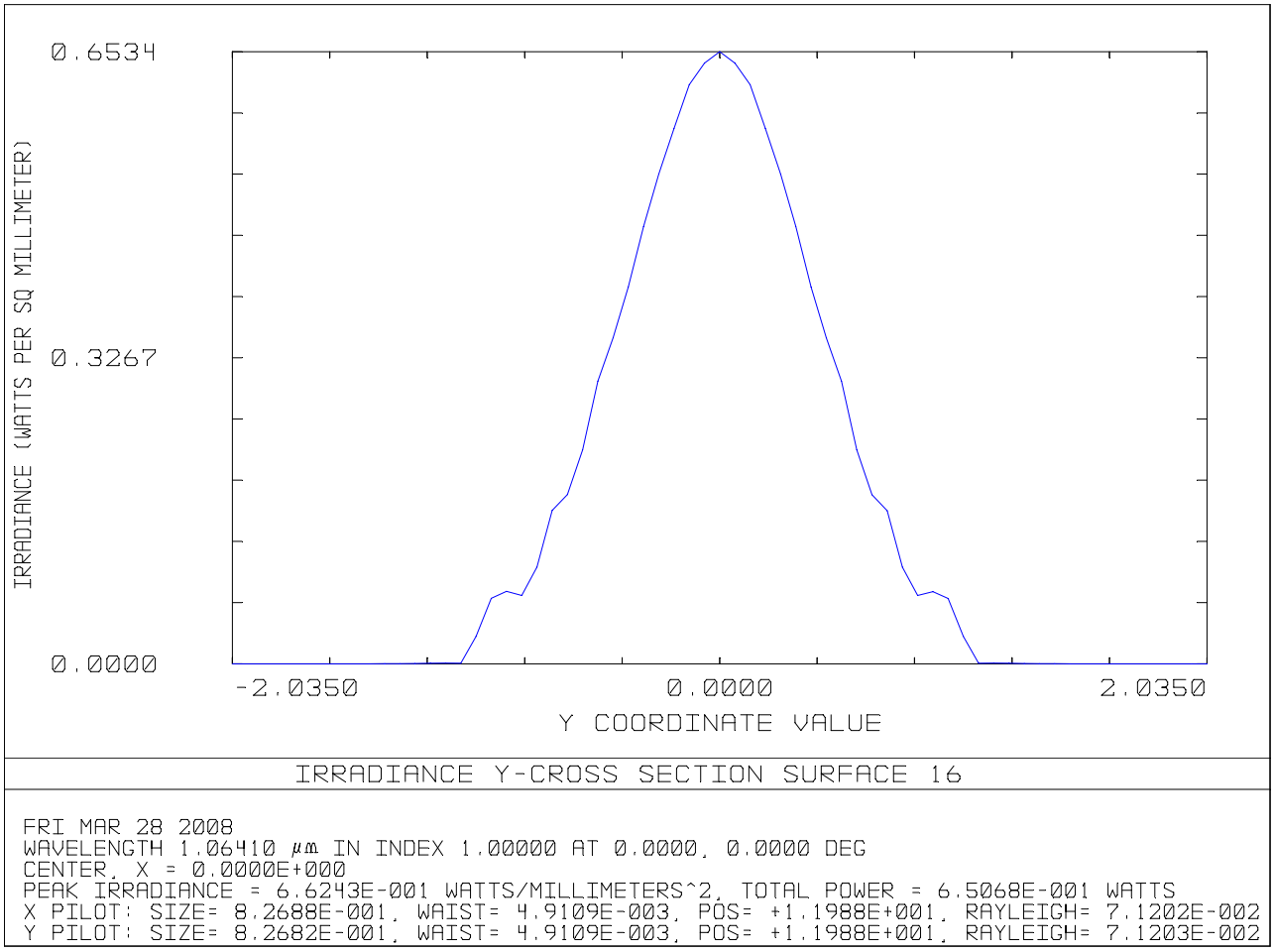

Figure 15: On-axis spot, Y Cross Section, 0.6 Waves Comatic Distortion

3.3.1.2 Off-axis, 4 mm

3.3.1.2.1 X Cross Section

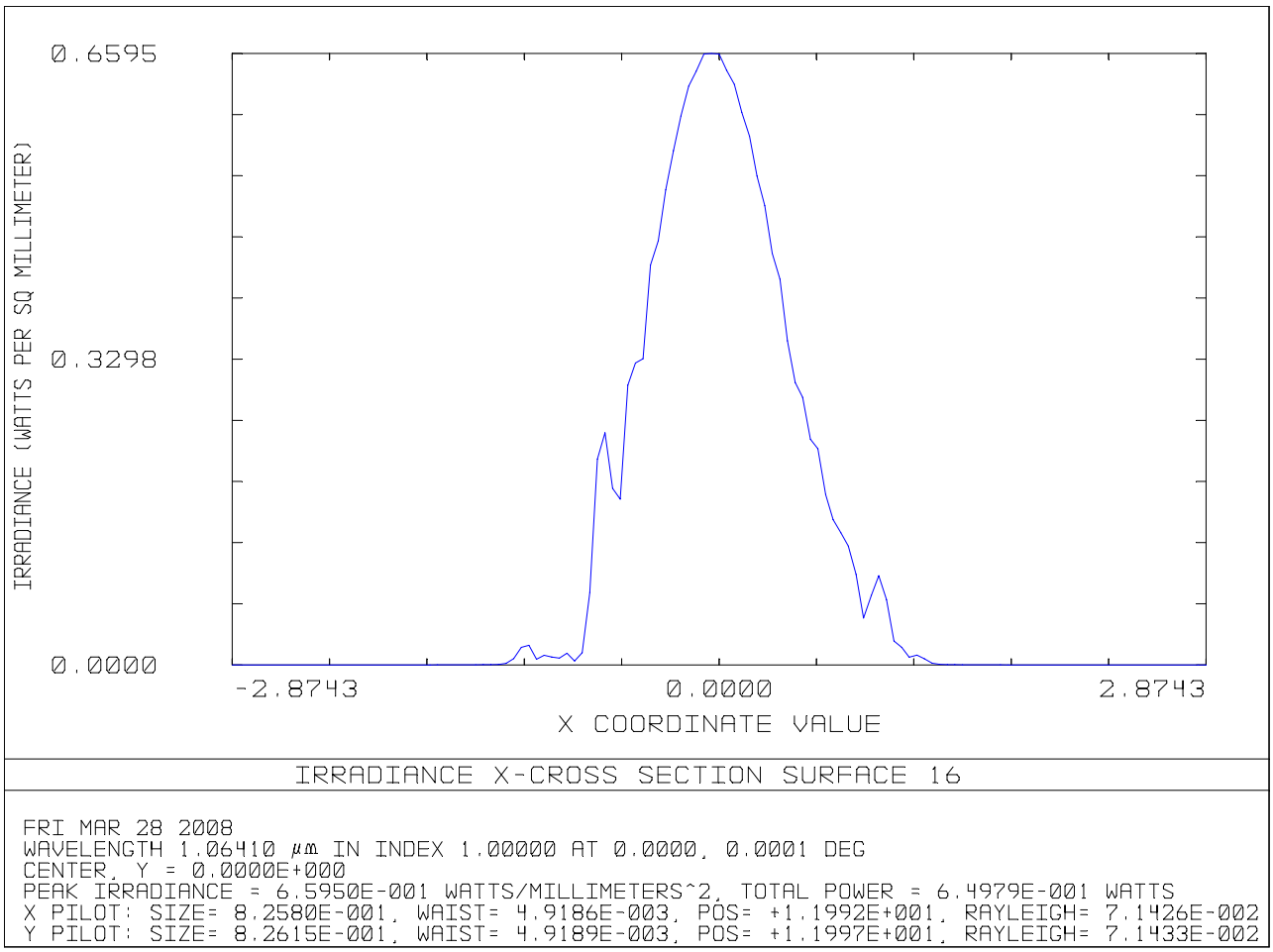

Figure 16: Off-axis 4 mm spot, X Cross Section, 0.6 Waves Comatic Distortion

3.3.1.2.2 Y Cross Section

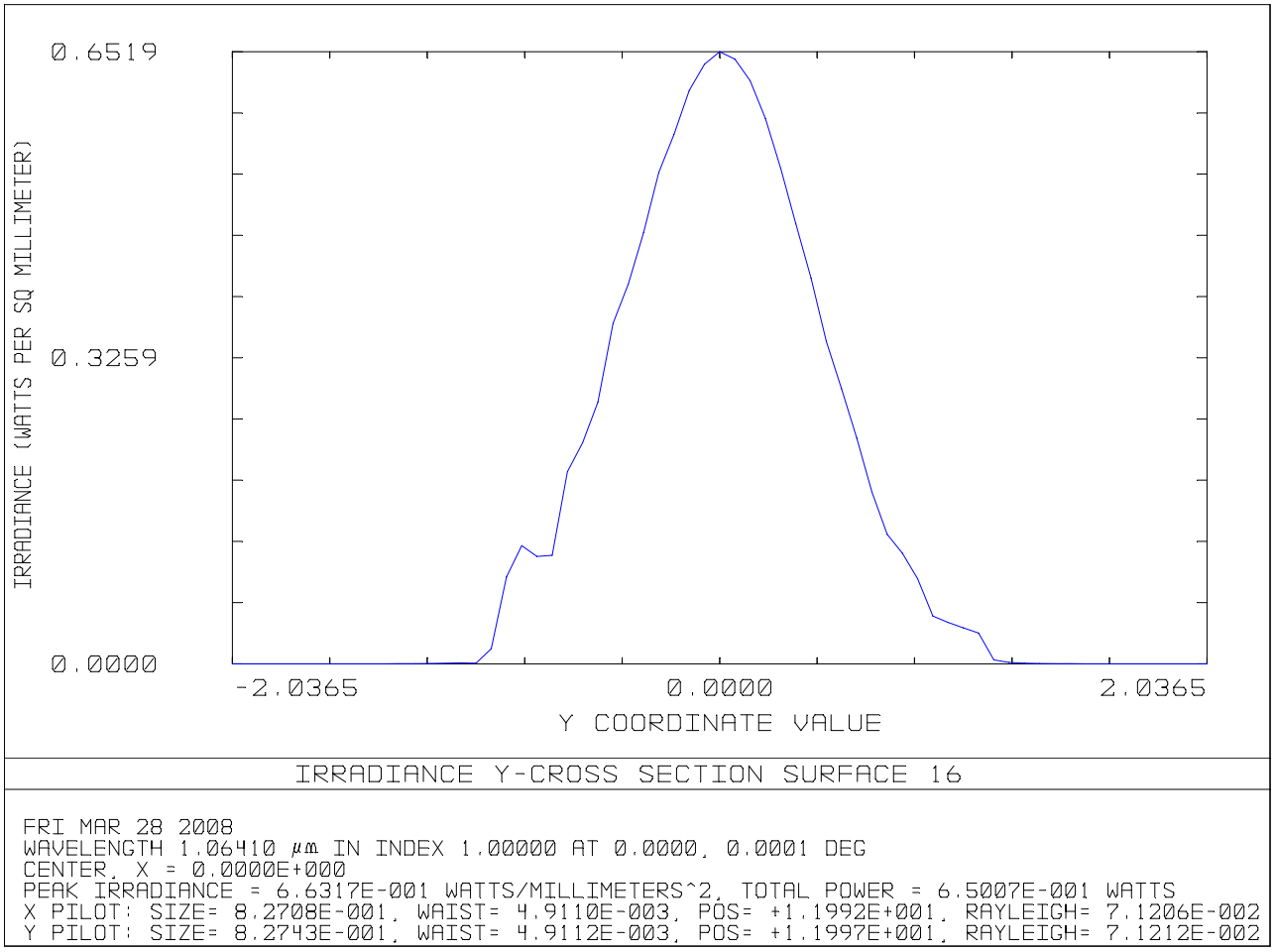

Figure 17: Off-axis 4 mm spot, Y Cross Section, 0.6 Waves Comatic Distortion

3.3.2 1.25 Waves of Comatic Phase Distortion

Note in the following figures that the distortion of the spot shape does not vary significantly for the three field positions.

3.3.2.1 On-Axis Beam

3.3.2.1.1 X Cross Section

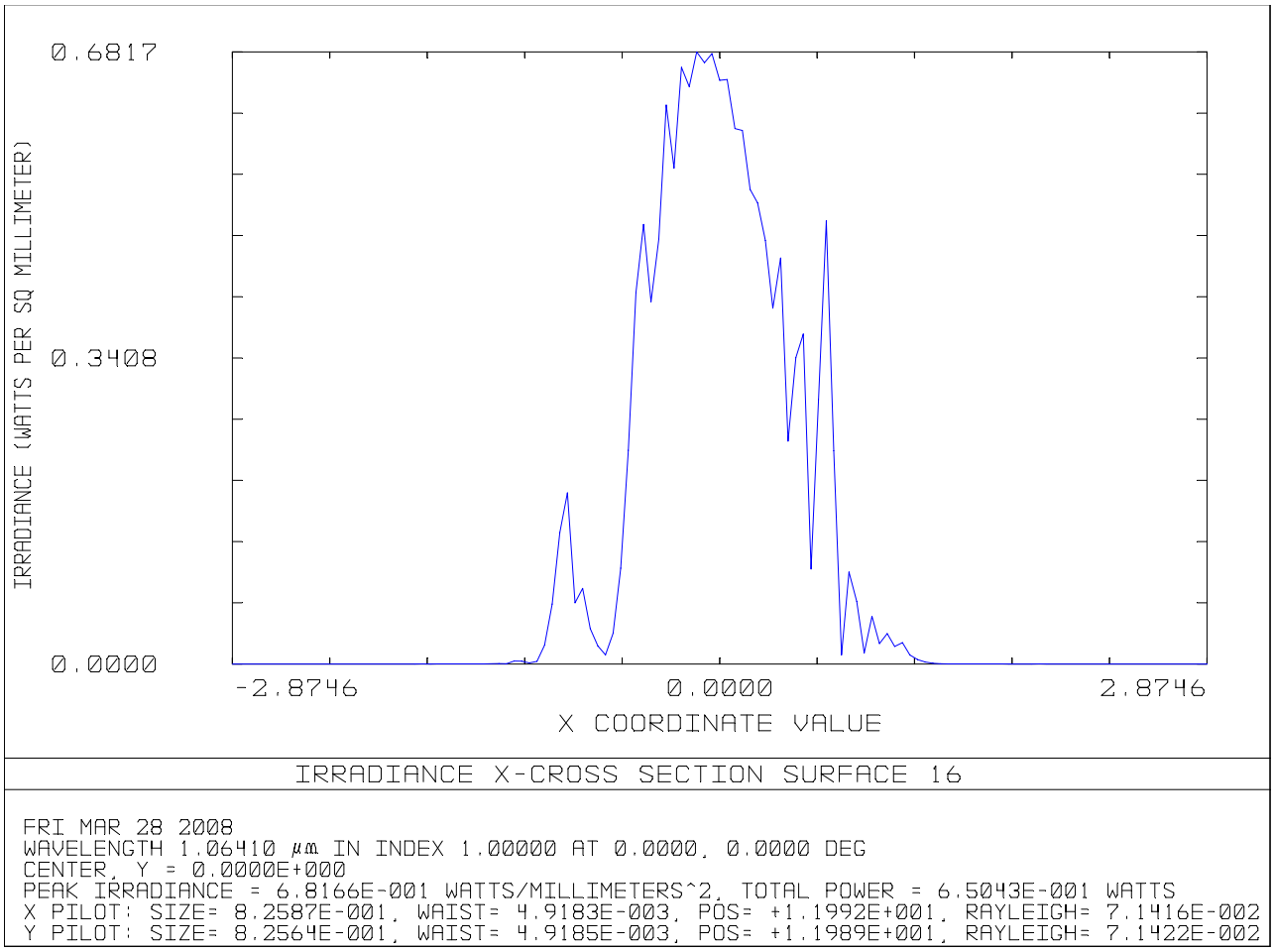

Figure 18: On-axis spot, X Cross Section, 1.25 Waves Comatic Distortion

3.3.2.1.2 Y Cross Section

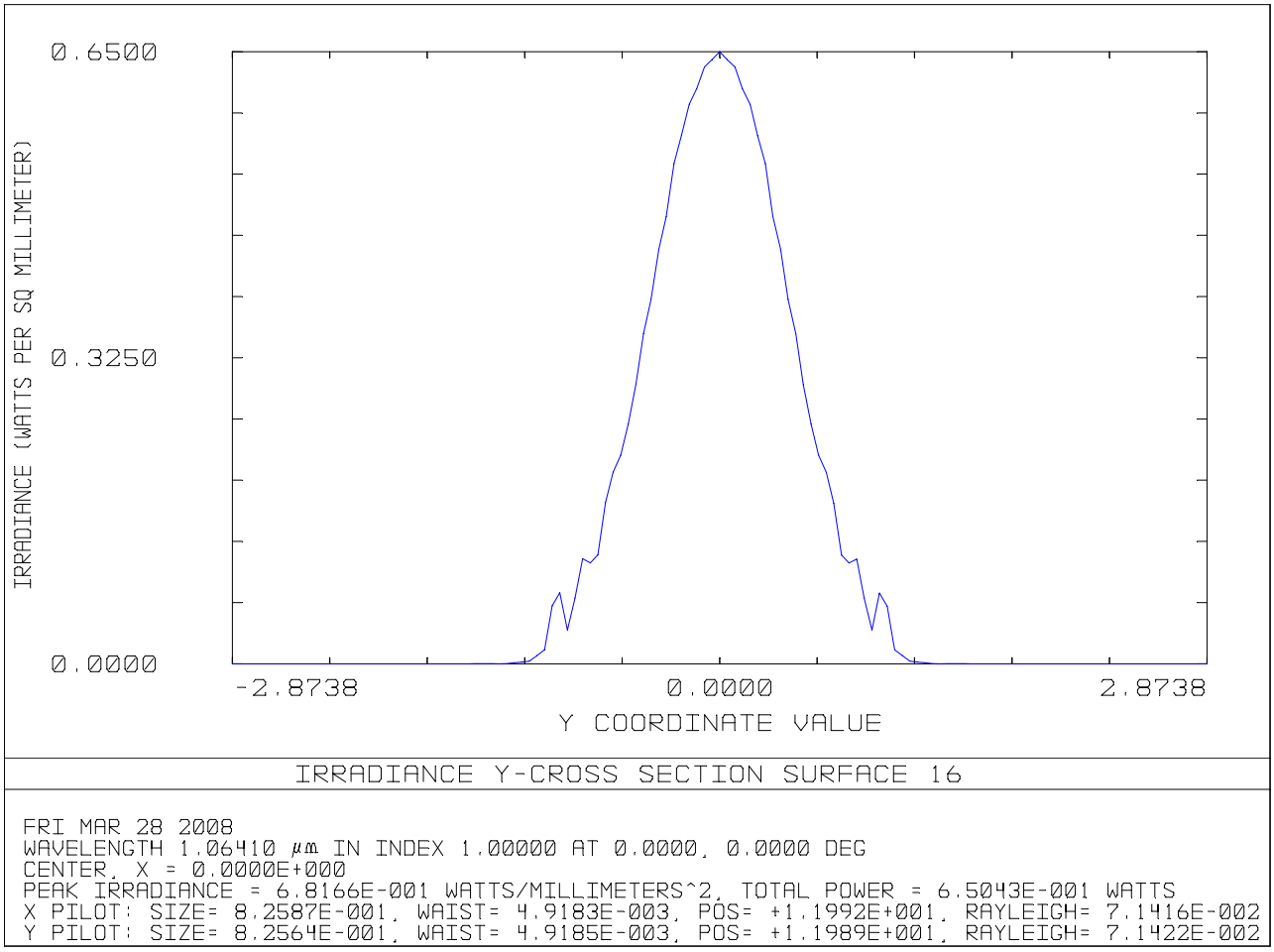

Figure 19: On-axis spot, Y Cross Section, 1.25 Waves Comatic Distortion

3.3.2.2 Off-axis, 4 mm

3.3.2.2.1 X Cross Section

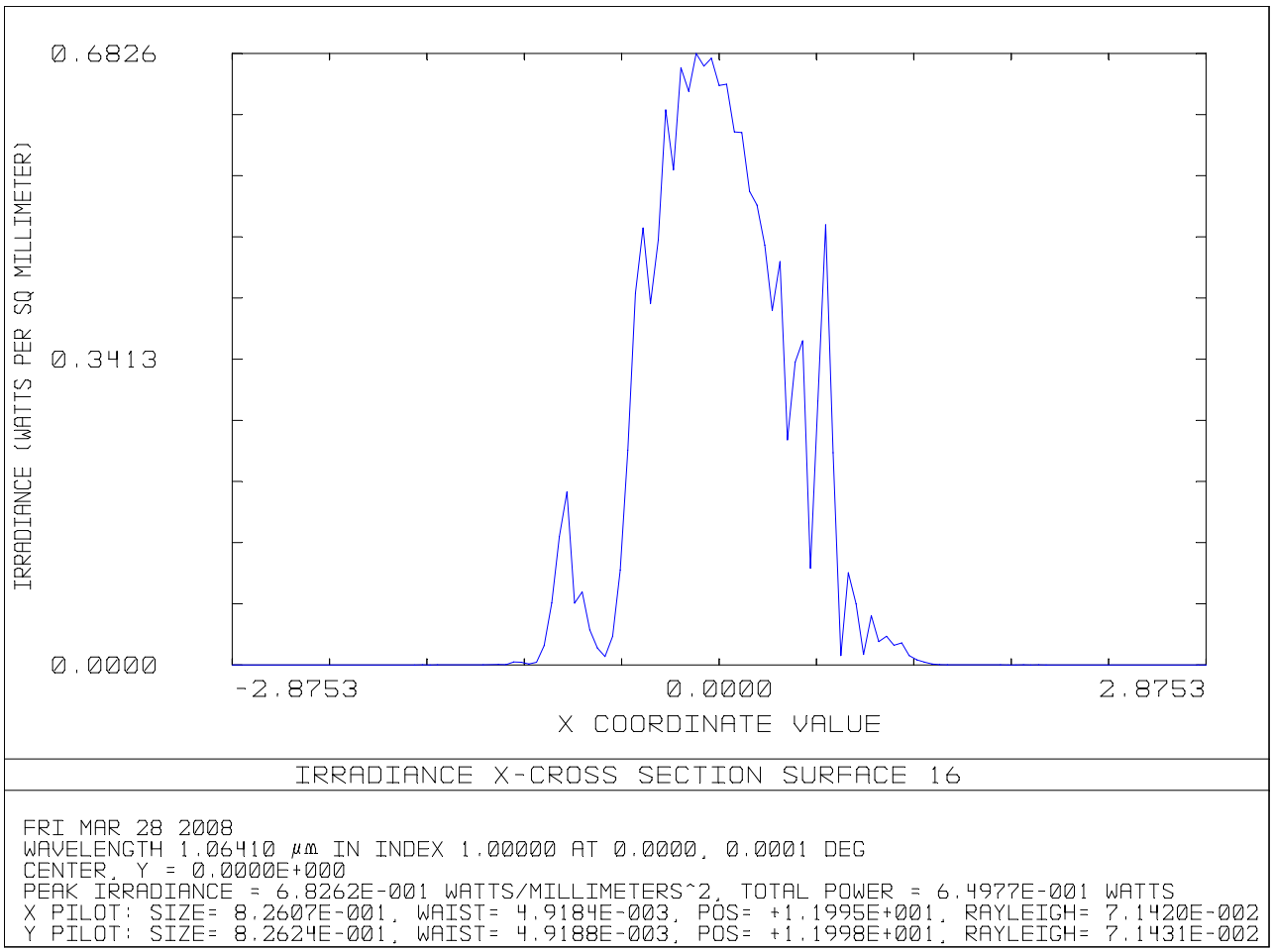

Figure 20: Off-axis 4 mm spot, X Cross Section, 1.25 Waves Comatic Distortion

3.3.2.2.2 Y Cross Section

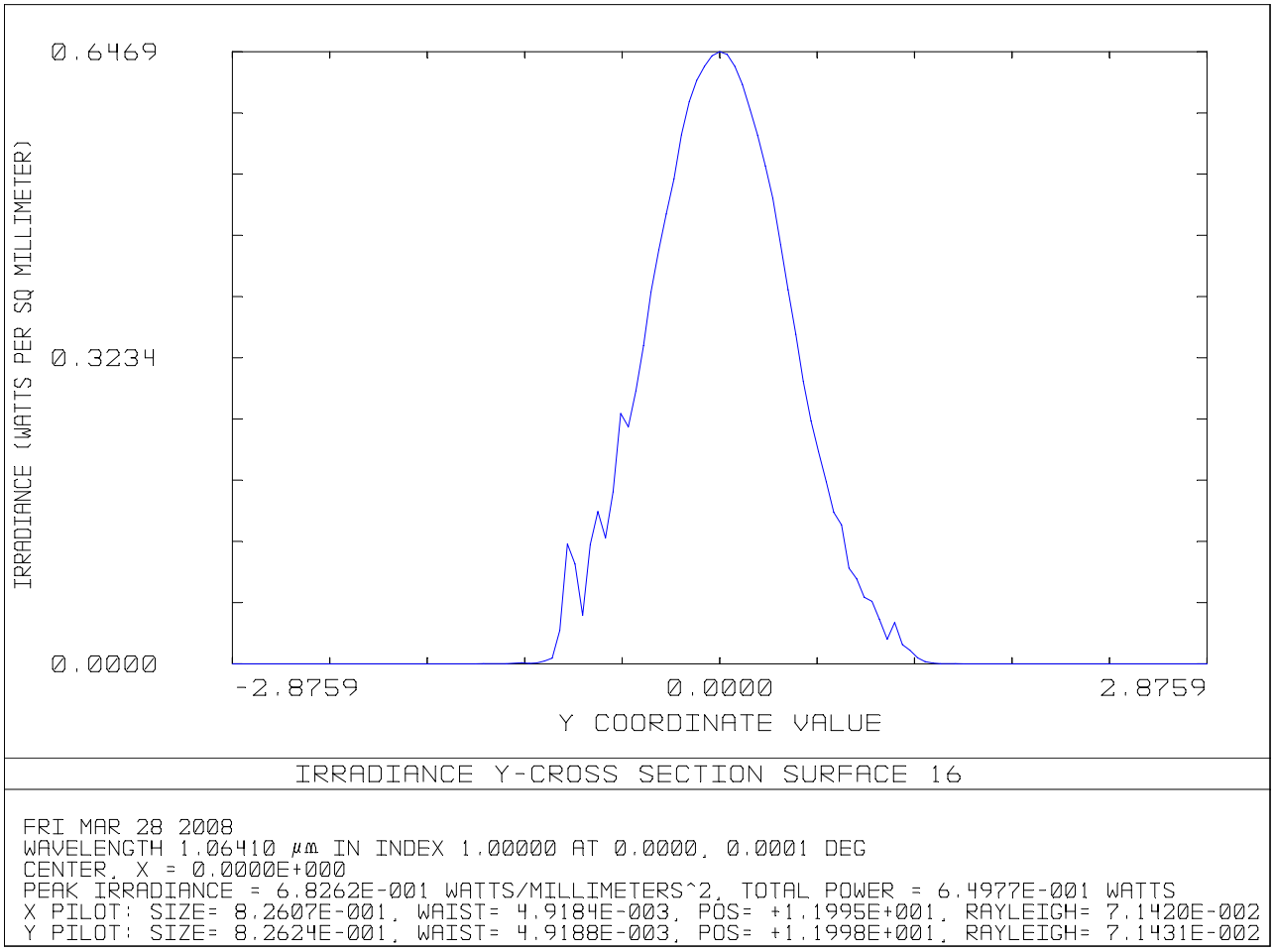

Figure 21: Off-axis 4 mm spot, Y Cross Section, 1.25 Waves Comatic Distortion

3.4 Effects of Combined Astigmatism and Coma on the Output Spot Shape

3.4.1 1.25 Waves of Astigmatic Plus 1.25 Waves of Comatic Phase Distortion, with 0 Deg Relative Azimuthal Angle

The following in-phase Zernike polynomials for astigmatism and coma were combined on the surface of the reaction mass (see Zemax Optical Design Program, Zemax Development Corp; Zernike Standard Polynomials):

$\sqrt{6}\cdot\left(\rho^2\cdot\cos(2\phi)\right)$ 0 deg relative azimuthal angle

$\sqrt{8}\cdot\left(3\cdot\rho^3-2\cdot\rho\right)\cdot\cos(\phi)$ 0 deg relative azimuthal angle

Note in the following figures that the distortion of the spot shape does not vary significantly for the three field positions.

3.4.1.1 On-axis

3.4.1.1.1 X Cross Section

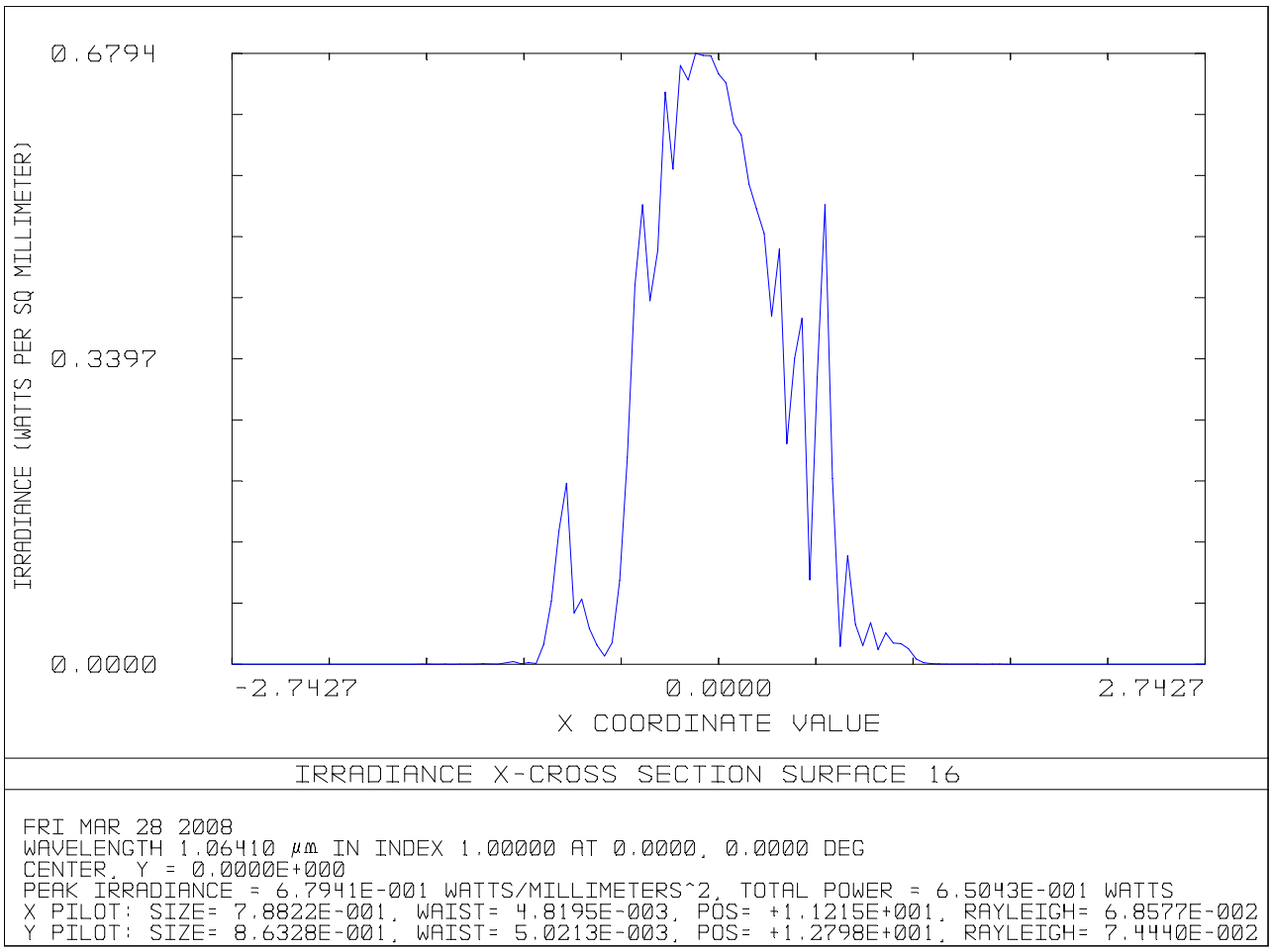

Figure 22: On-axis spot, X Cross Section, 1.25 Waves Astigmatic plus 1.25 Waves Comatic Distortion, 0 Deg Relative Azimuthal Angle

3.4.1.1.2 Y Cross Section

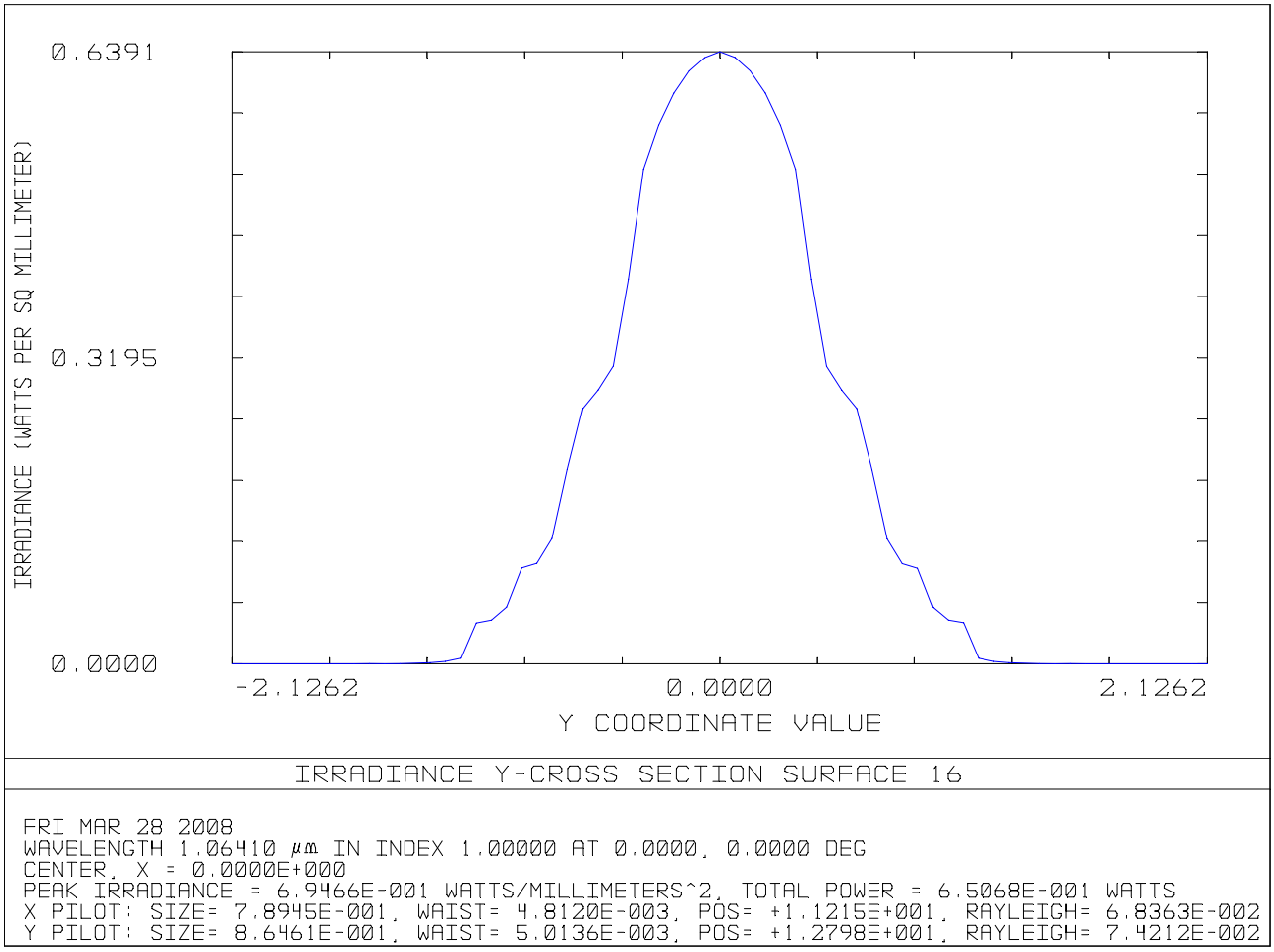

Figure 23: On-axis spot, Y Cross Section, 1.25 Waves Astigmatic plus 1.25 Waves Comatic Distortion, 0 Deg Relative Azimuthal Angle

3.4.1.2 Off-axis, 4 mm

3.4.1.2.1 X Cross Section

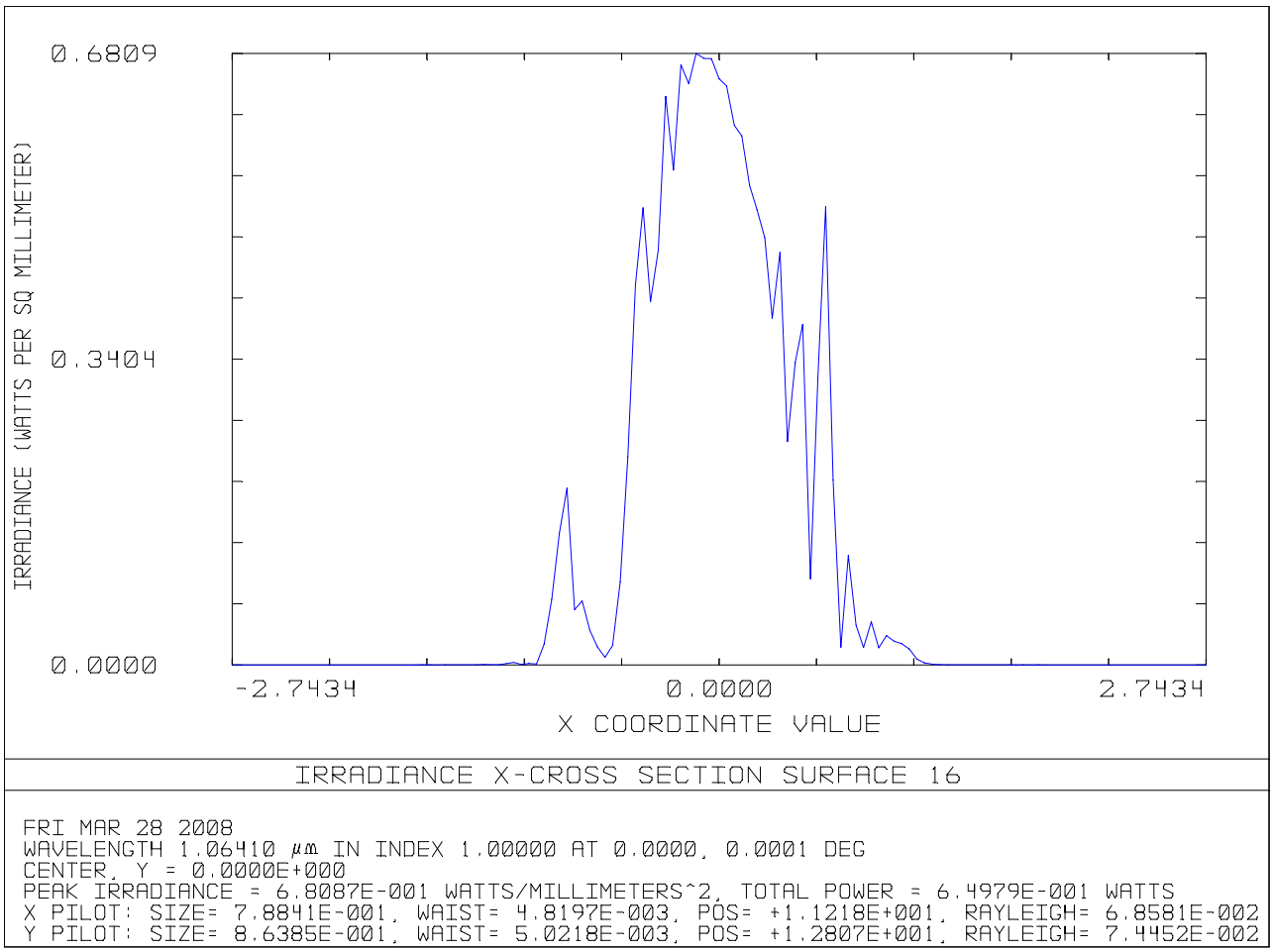

Figure 24: Off-axis 4 mm spot, X Cross Section, 1.25 Waves Astigmatic plus 1.25 Waves Comatic Distortion, 0 Deg Relative Azimuthal Angle

3.4.1.2.2 Y Cross Section

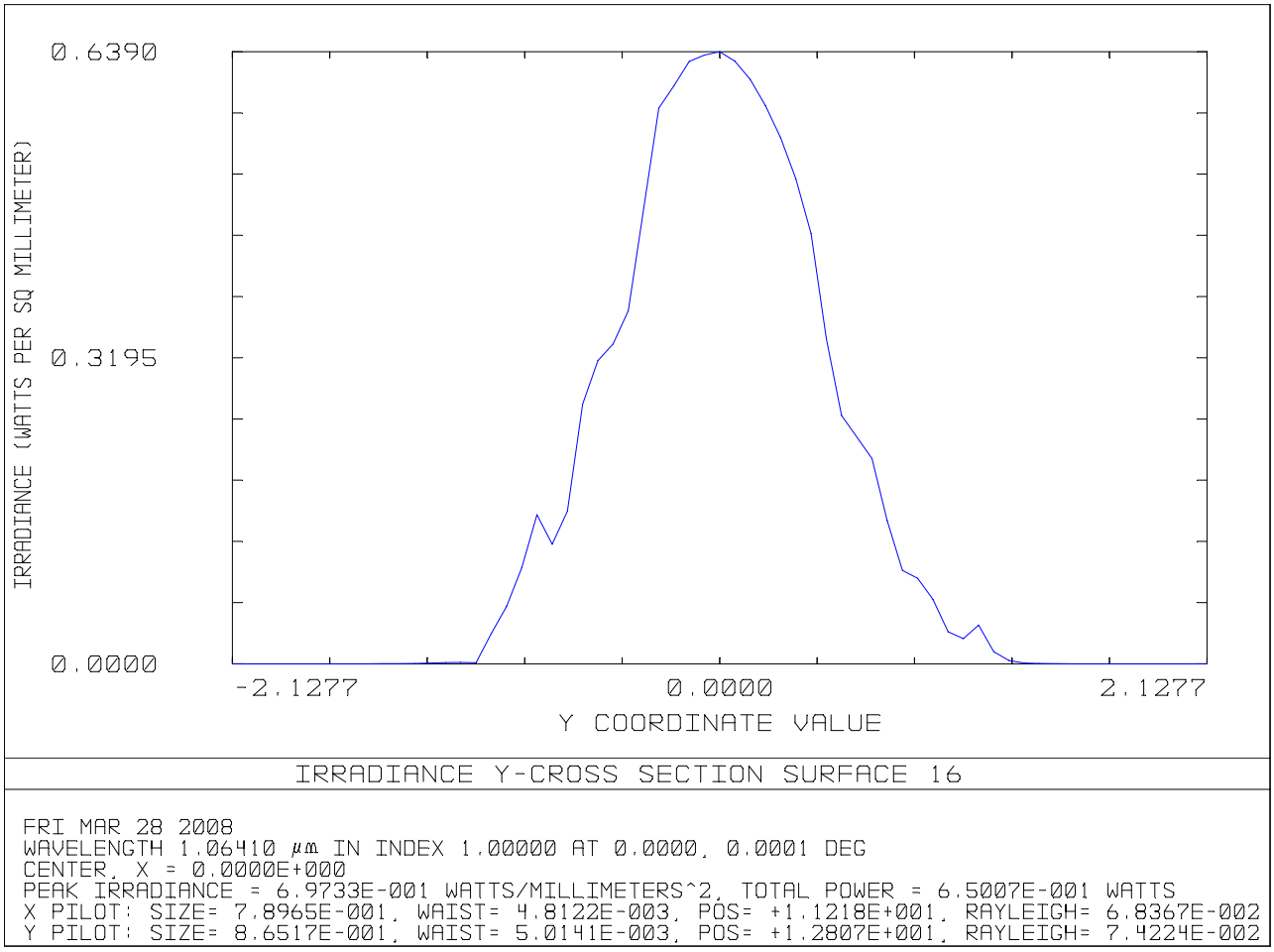

Figure 25: Off-axis 4 mm spot, Y Cross Section, 1.25 Waves Astigmatic plus 1.25 Waves Comatic Distortion, 0 Deg Relative Azimuthal Angle

3.4.2 1.25 Waves of Astigmatic Plus 1.25 Waves of Comatic Phase Distortion, with 90 deg Relative Azimuthal Angle

The following out-of-phase Zernike polynomials for astigmatism and coma were combined on the surface (see Zemax Optical Design Program, Zemax Development Corp; Zernike Standard Polynomials):

$\sqrt{6}\cdot\left(\rho^2\cdot\sin(2\phi)\right)$ 90 deg relative azimuthal angle

$\sqrt{8}\cdot\left(3\cdot\rho^3-2\cdot\rho\right)\cdot\cos(\phi)$ 0 deg relative azimuthal angle

Note in the following figures that the distortion of the spot shape does not vary significantly for the three field positions.

3.4.2.1 On-axis

3.4.2.1.1 X Cross Section

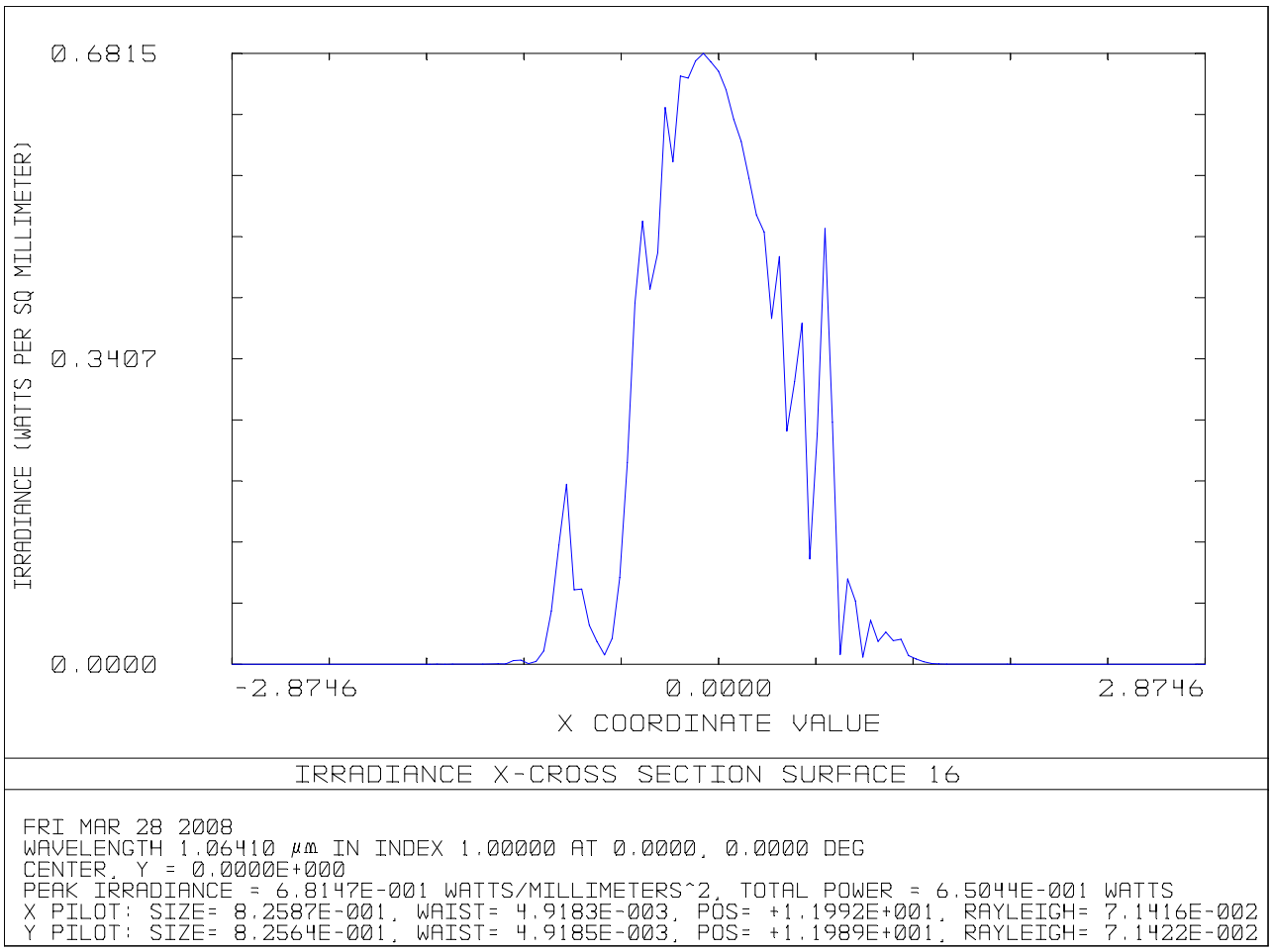

Figure 26: On-axis spot, X Cross Section, 1.25 Waves Astigmatic plus 1.25 Waves Comatic Distortion, 90 Deg Relative Azimuthal Angle

3.4.2.1.2 Y Cross Section

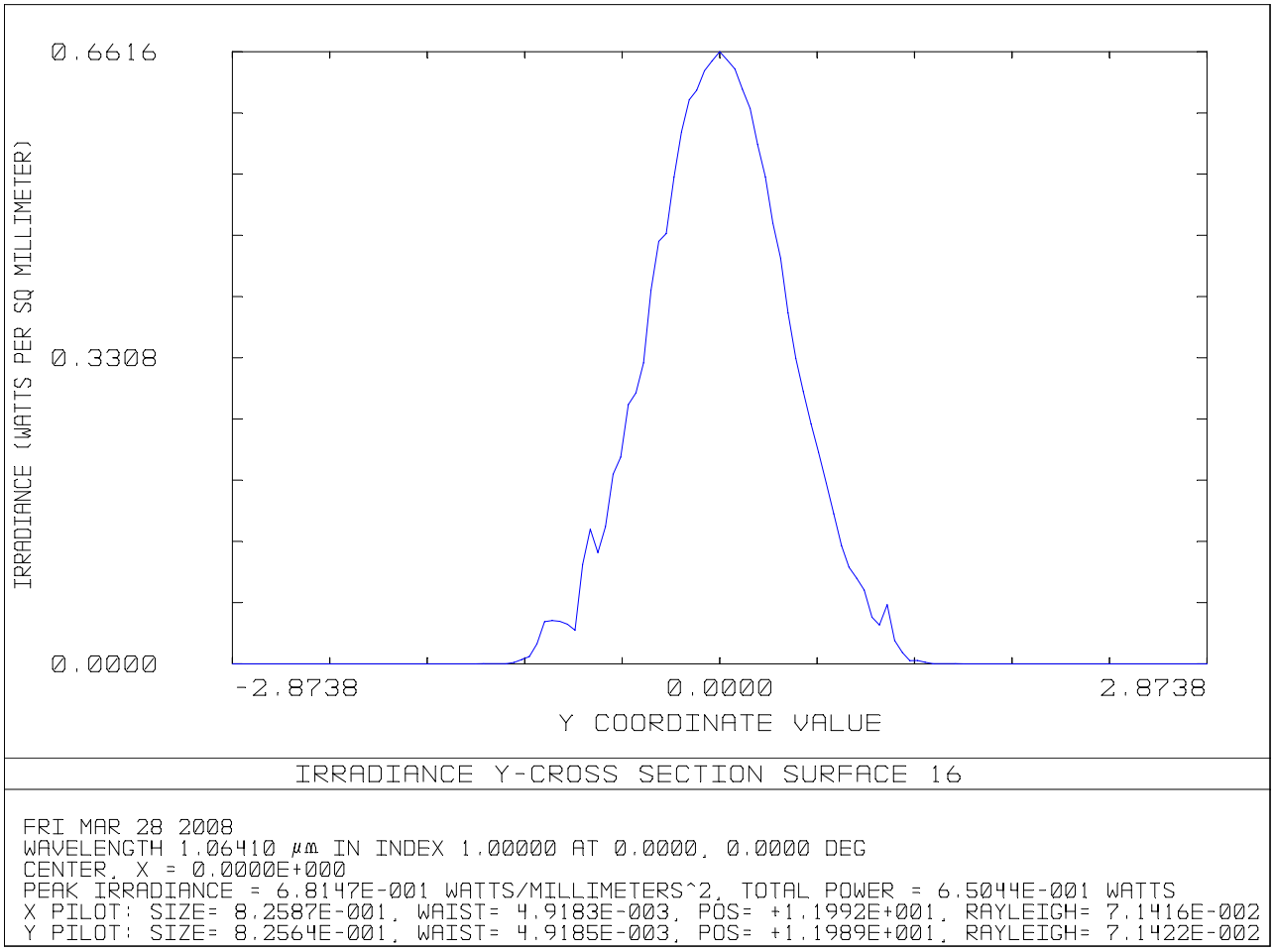

Figure 27: On-axis spot, Y Cross Section, 1.25 Waves Astigmatic plus 1.25 Waves Comatic Distortion, 90 Deg Relative Azimuthal Angle

3.4.2.2 Off-axis, 4 mm

3.4.2.2.1 X Cross Section

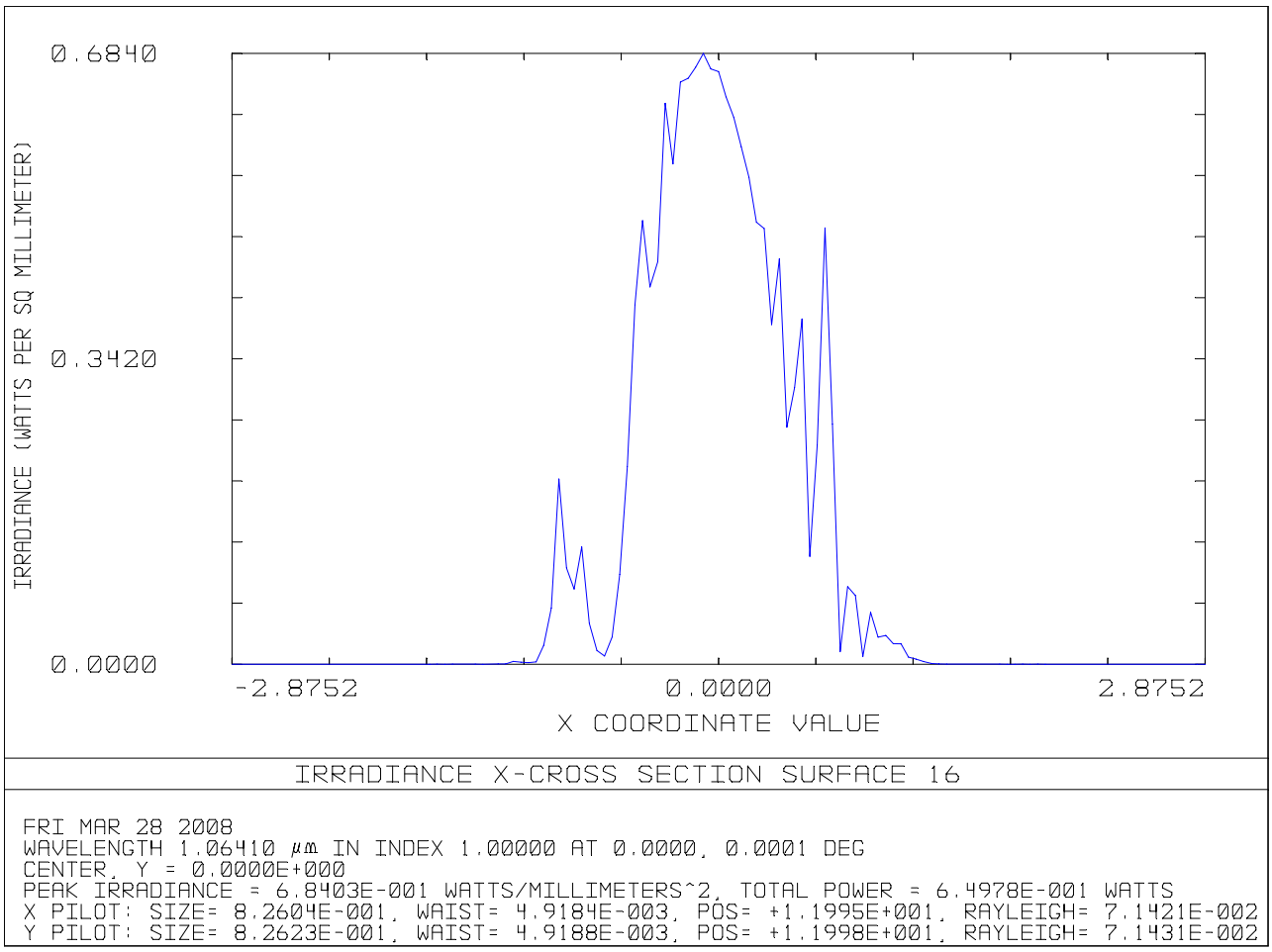

Figure 28: Off-axis 4 mm spot, X Cross Section, 1.25 Waves Astigmatic plus 1.25 Waves Comatic Distortion, 90 Deg Relative Azimuthal Angle

3.4.2.2.2 Y Cross Section

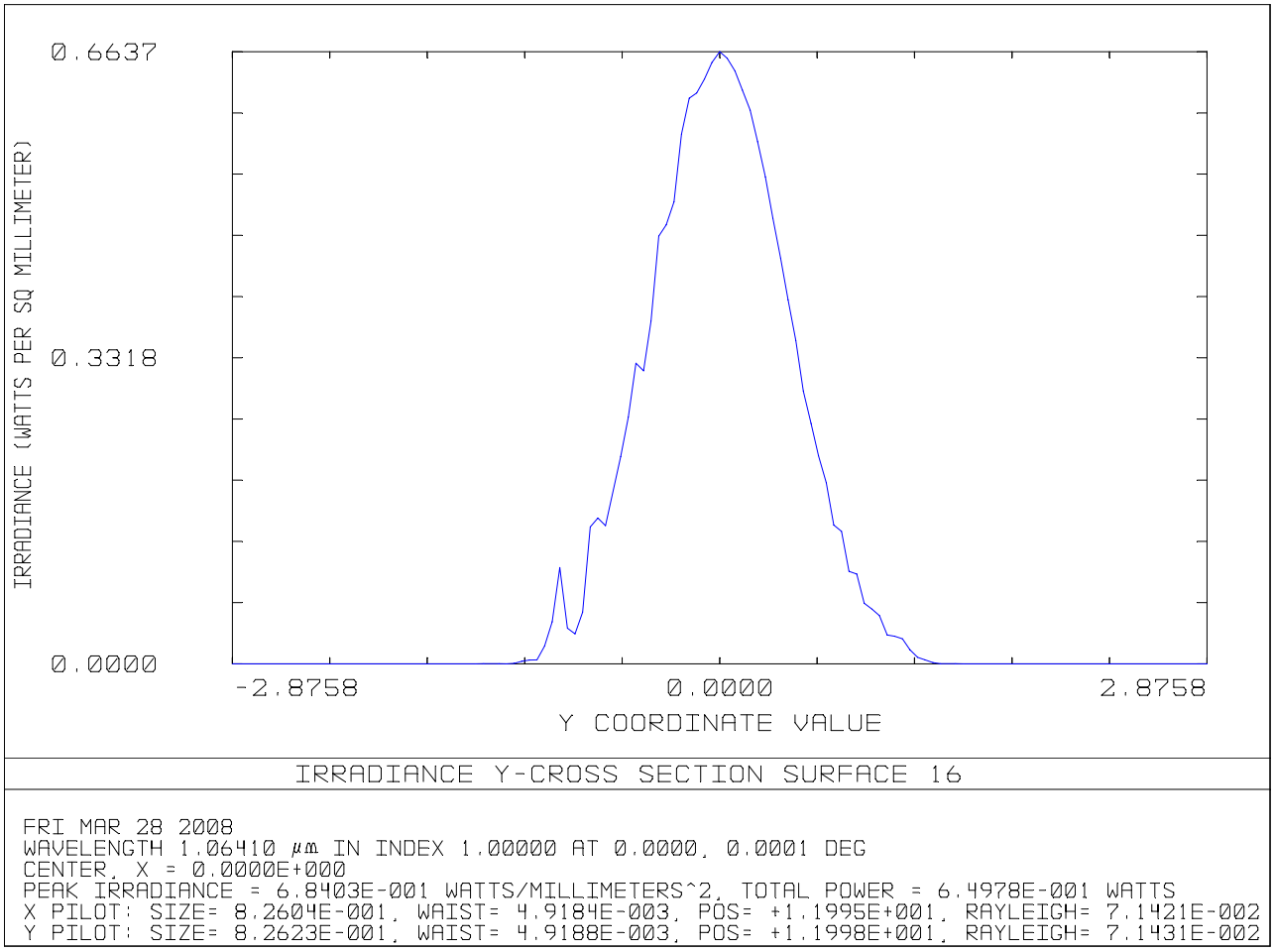

Figure 29: Off-axis 4 mm spot, Y Cross Section, 1.25 Waves Astigmatic plus 1.25 Waves Comatic Distortion, 90 Deg Relative Azimuthal Angle

3.4.3 0.25 Waves of High Order Distortion

The following high order polynomial with an azimuthal angle multiple of 6 was chosen, to simulate a lumpiness in the distortion with a spatial dimension of approximately 84 mm at the periphery of the 180 mm clear aperture. (see Zemax Optical Design Program, Zemax Development Corp; Zernike Standard Polynomials):

$$\sqrt{14}\cdot\left(\rho^{6}\cdot\cos(6\phi)\right)$$

Note in the following figures that the distortion of the spot shape does not vary significantly for the three field positions.

3.4.3.1 On-axis

3.4.3.1.1 X Cross Section

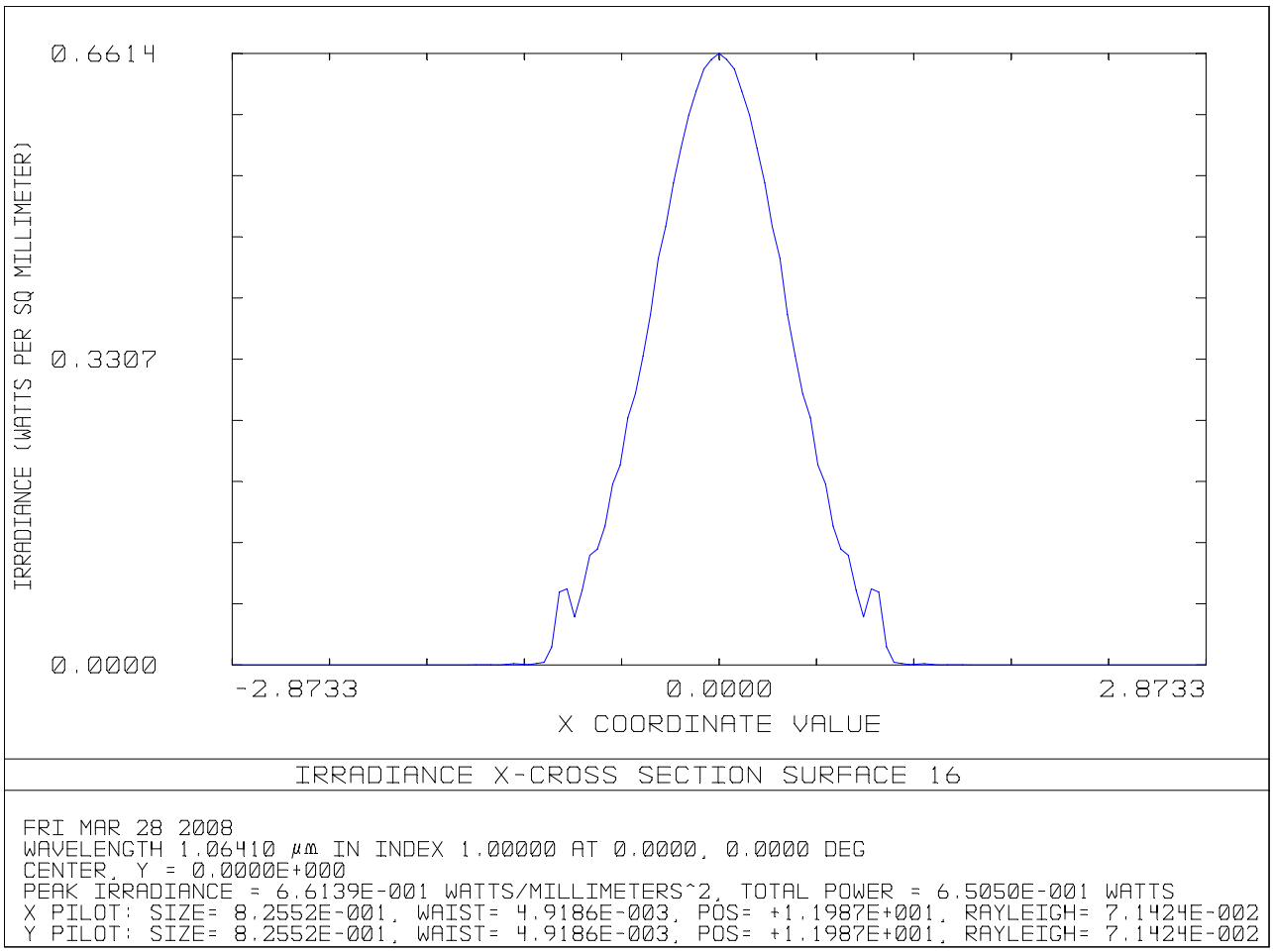

Figure 30: On-axis spot, X Cross Section, 0.25 Waves High Order Distortion

3.4.3.1.2 Y Cross Section

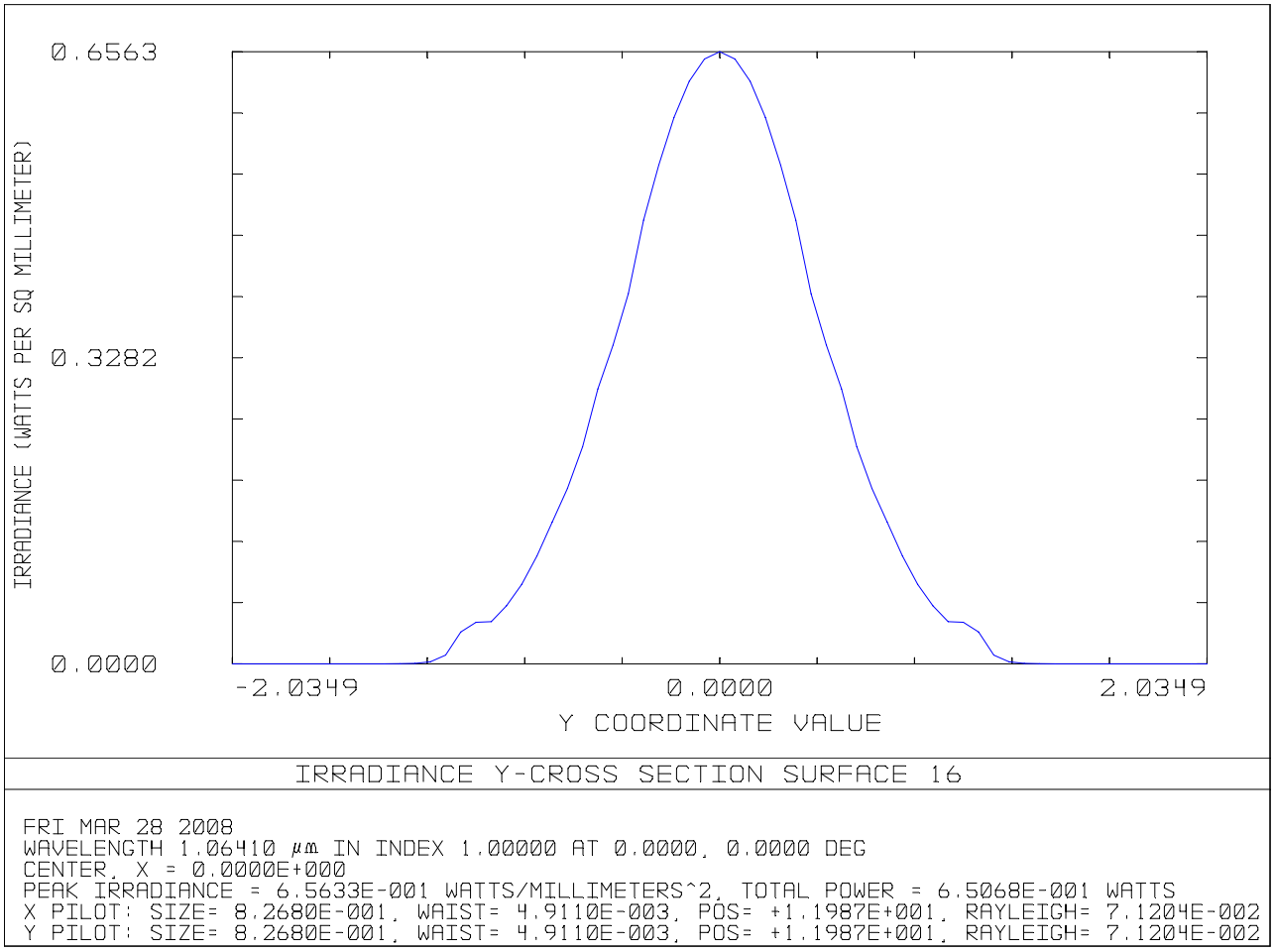

Figure 31: On-axis spot, Y Cross Section, 0.25 Waves High Order Distortion

3.4.3.2 Off-axis, 4 mm

3.4.3.2.1 X Cross Section

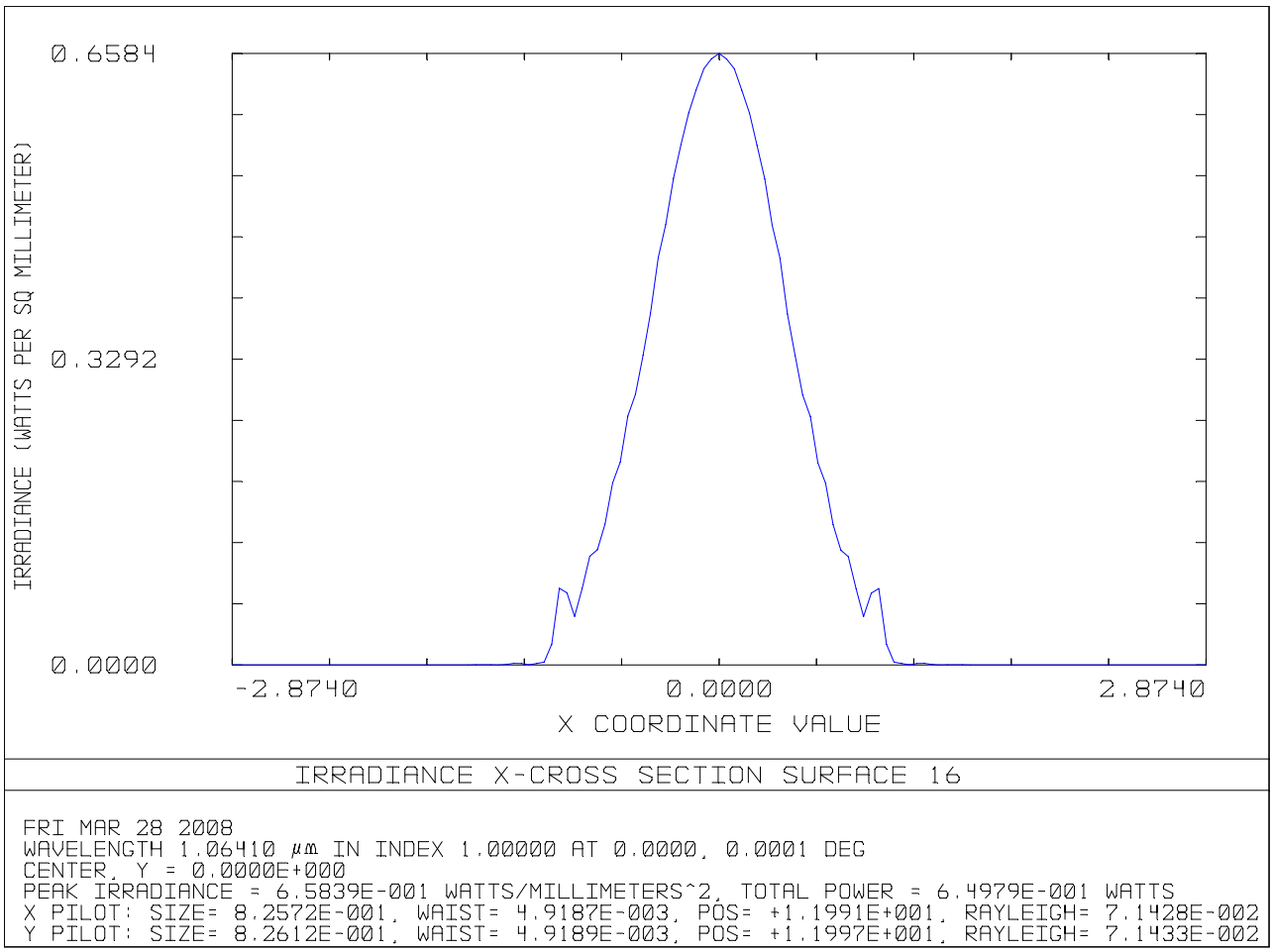

Figure 32: Off-axis 4 mm spot, X Cross Section, 0.25 Waves High Order Distortion

3.4.3.2.2 Y Cross Section

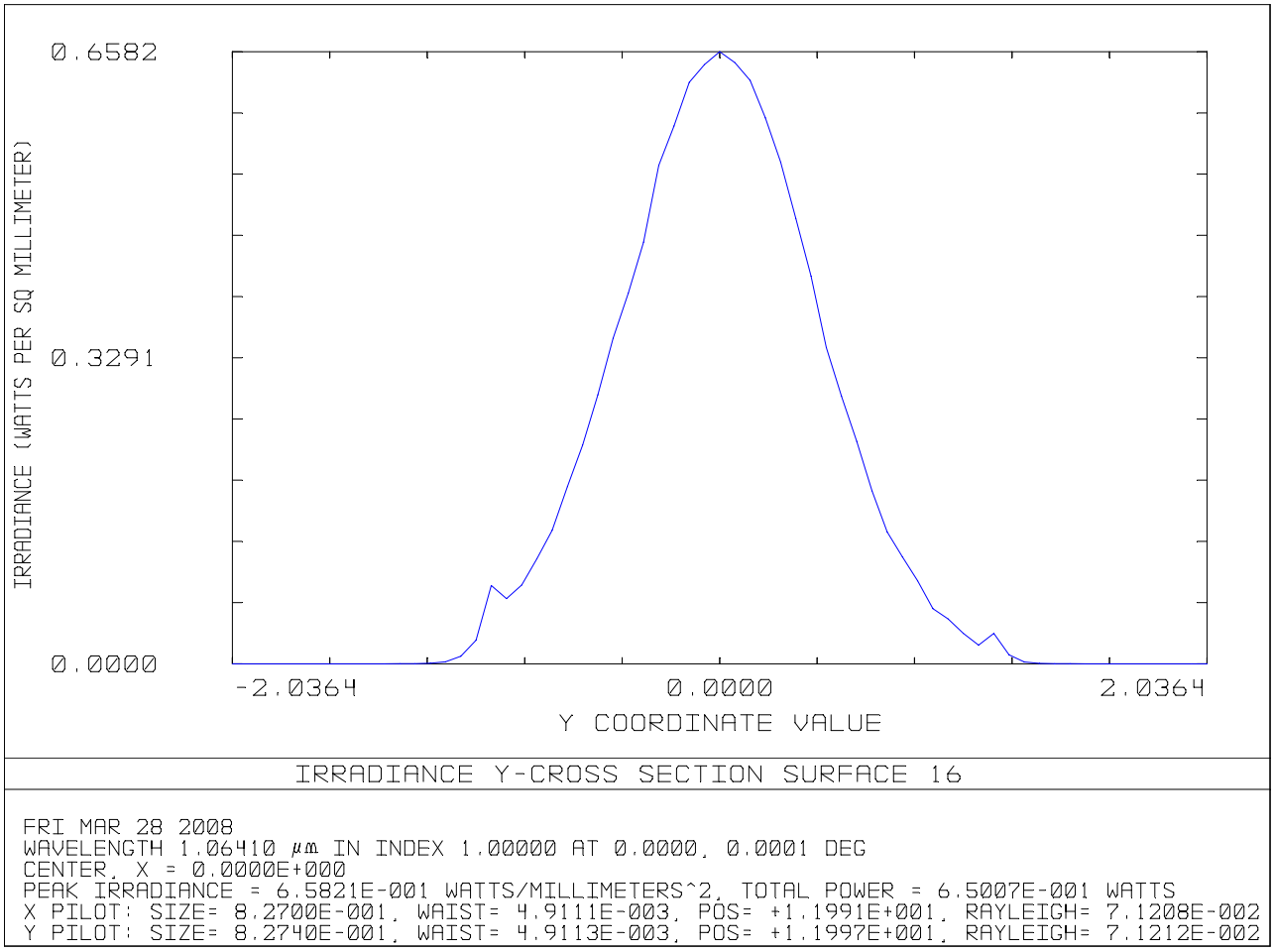

Figure 33: Off-axis 4 mm spot, Y Cross Section, 0.25 Waves High Order Distortion

3.5 Effects of Astigmatism on the Output Spot Centroid Displacement

The X, Y positions of the output spot centroid at the plane of the QPD with a Y displacement at the ETM was calculated by Zemax for the three field displacements; on-axis, 2 mm, and 4 mm off-axis, using the RMS spot radius centroid merit function.

It can be seen that the Y position on the QPD varies approximately linearly with field displacement, and the amplitude is essentially in-dependent on the magnitude of phase distortion.

In this case the X offset is zero.

3.5.1 Y Centroid Displacement at QPD

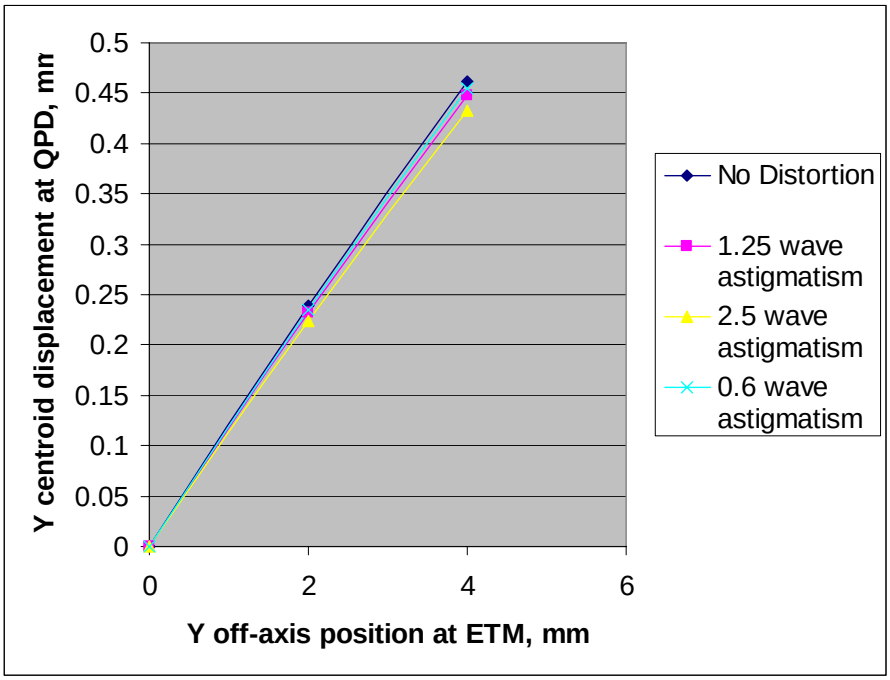

Figure 34: Y Centroid Displacement at QPD, Astigmatic Distortion

3.5.2 X Centroid Displacement at QPD

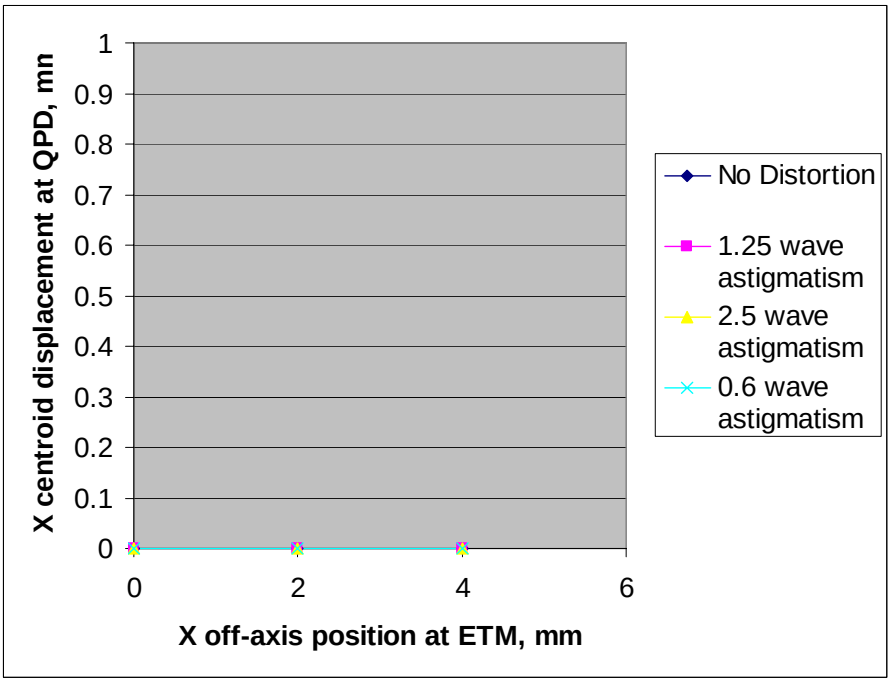

Figure 35: X Centroid Displacement at QPD, Astigmatic Distortion

3.6 Effects of Coma on the Output Spot Centroid Displacement

The X, Y positions of the output spot centroid at the plane of the QPD with a Y displacement at the ETM was calculated by Zemax for the three field displacements; on-axis, 2 mm, and 4 mm off-axis.

In this case, the following Zernike coma polynomial with azimuthal angle shifted by 90 deg was used,

$$\sqrt{8}\cdot\left(3\cdot\rho^{3}-2\cdot\rho\right)\cdot\sin(\phi)$$

which produced a Y offset for the on-axis field that increased with the magnitude of the distortion. The on-axis Y offset was subtracted from the Y data positions to demonstrate that the output beam spot could be pre-aligned on the QPD.

After subtracting the constant Y on-axis offset, it can be seen that the Y position on the QPD varies linearly with field displacement.

In this case the X offset is zero.

3.6.1 Y Centroid Displacement at QPD

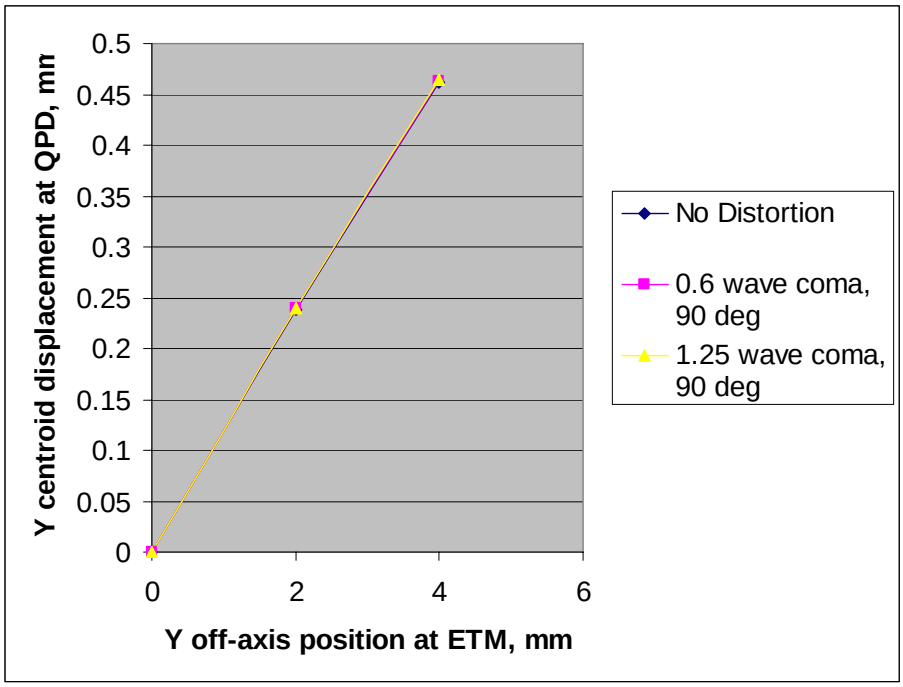

Figure 36: Y Centroid Displacement at QPD, Comatic Distortion

3.6.2 X Centroid Displacement at QPD

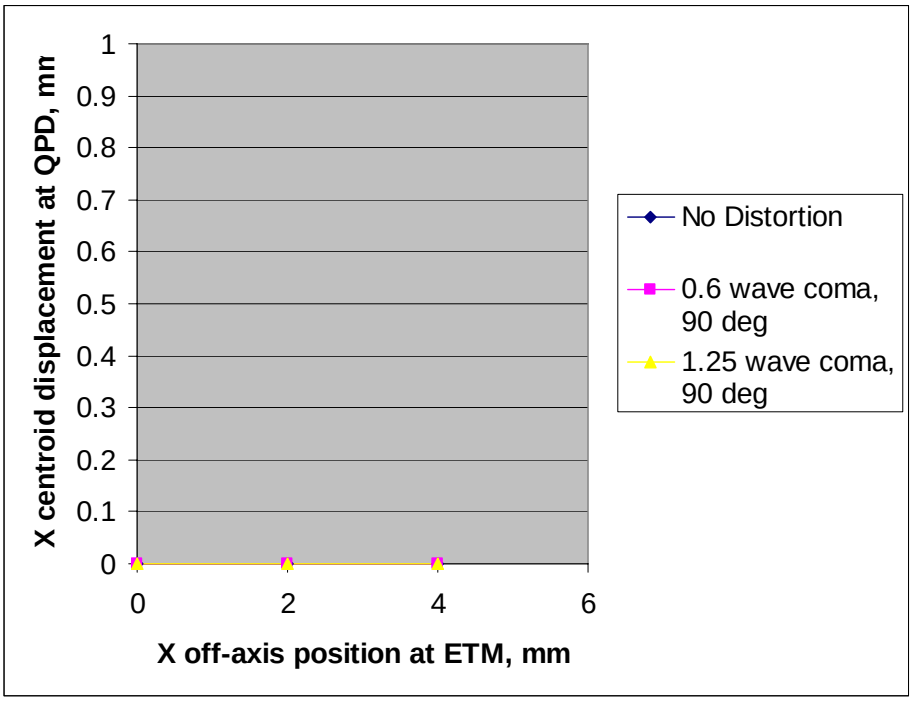

Figure 37: X Centroid Displacement at QPD, Comatic Distortion

3.7 Effects of Combined Astigmatism and Coma on the Output Spot Centroid Displacement

The X, Y positions of the output spot centroid at the plane of the QPD with a Y displacement at the ETM was calculated by Zemax for the three field displacements; on-axis, 2 mm, and 4 mm off-axis, using the RMS spot radius centroid merit function. In one case, the Zernike polynomials were added with the same azimuthal angle; and in the other, with a relative shift of 90 degrees between the azimuthal angles.

It can be seen that the Y position on the QPD varies approximately linearly with field displacement, and the amplitude is essentially in-dependent on the magnitude of phase distortion.

In this case the X offset is zero.

3.7.1 Y Centroid Displacement at QPD

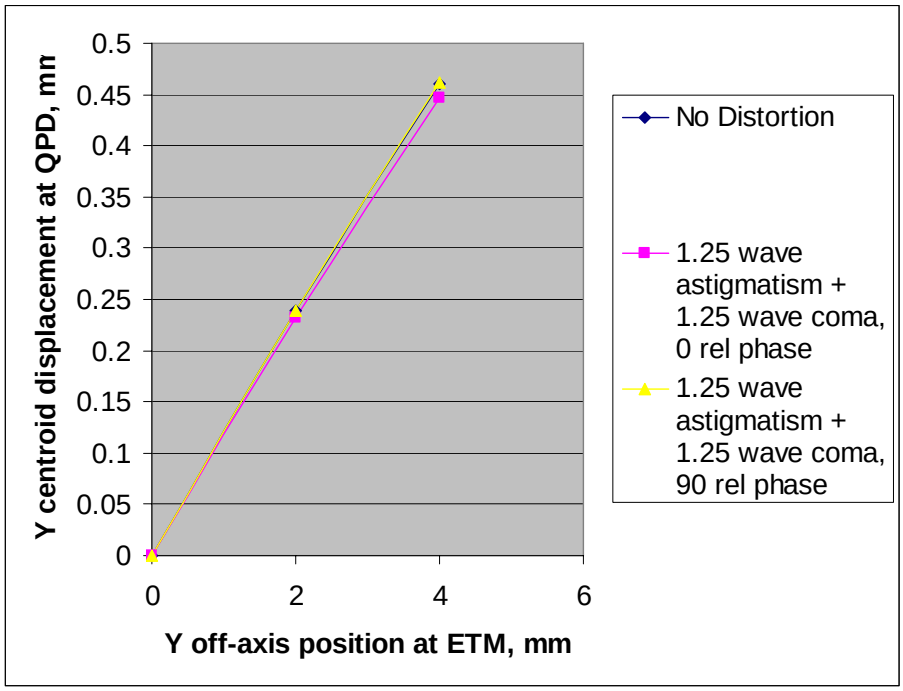

Figure 38: Y Centroid Displacement at QPD, Combined Astigmatic and Comatic Distortion

3.7.2 X Centroid Displacement at QPD

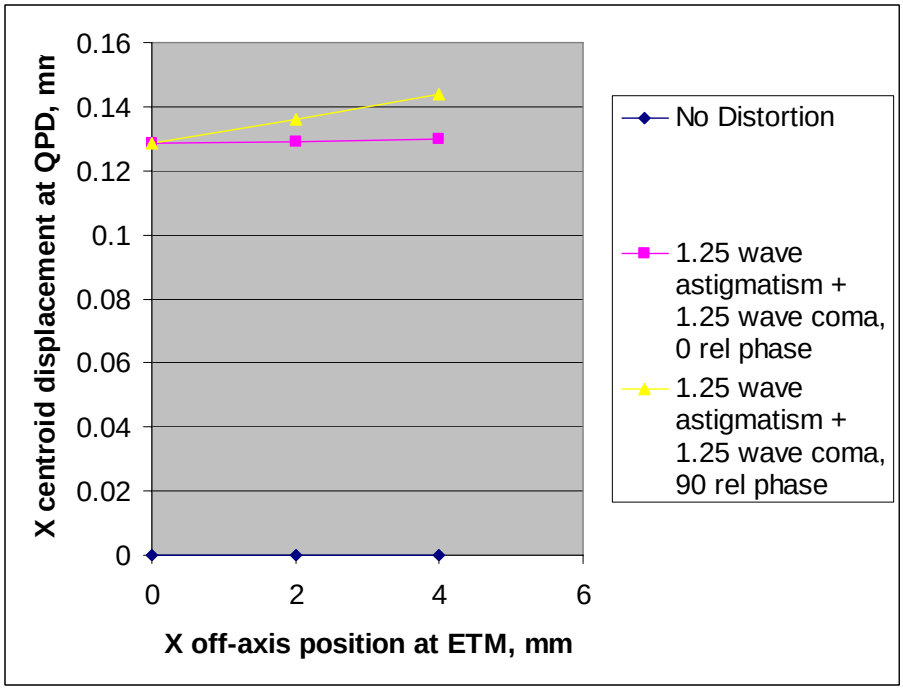

Figure 39: X Centroid Displacement at QPD, Combined Astigmatic and Comatic Distortion

3.8 Effects of High Order Distortion on the Output Spot Centroid Displacement

The X, Y positions of the output spot centroid at the plane of the QPD with a Y displacement at the ETM was calculated by Zemax for the three field displacements; on-axis, 2 mm, and 4 mm off-axis.

It can be seen that the Y position on the QPD varies approximately linearly with field displacement, and the amplitude is essentially in-dependent on the magnitude of phase distortion.

In this case the X offset is zero.

3.8.1 Y Centroid Displacement at QPD

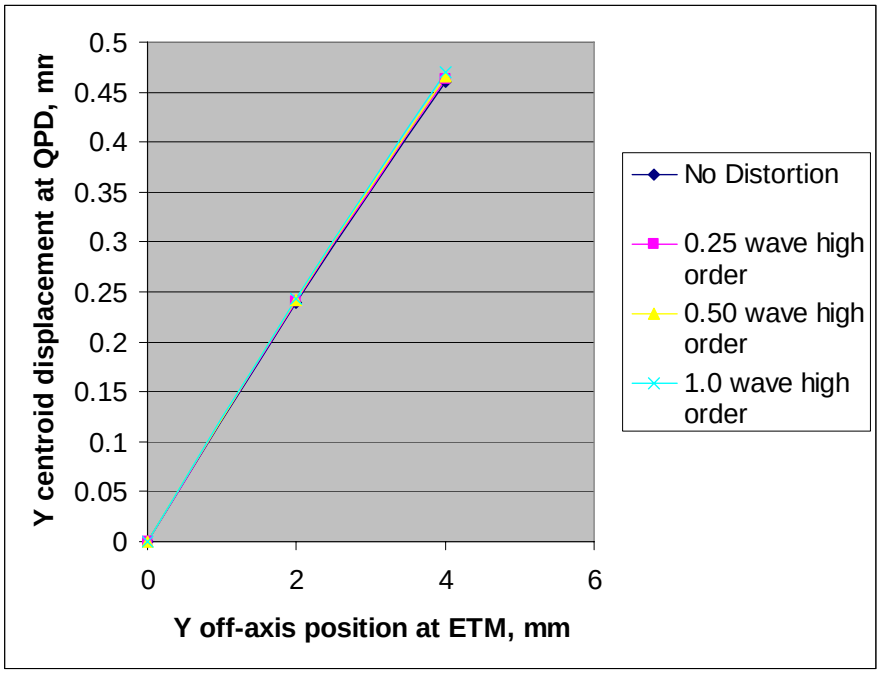

Figure 40: Y Centroid Displacement at QPD, High Order Distortion

3.8.2 X Centroid Displacement at QPD

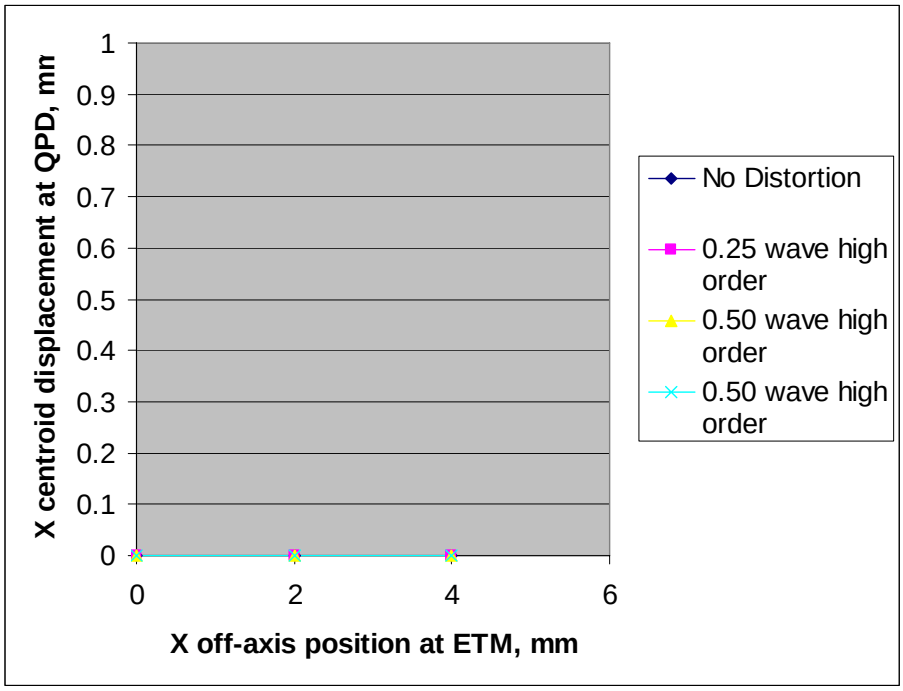

Figure 41: X Centroid Displacement at QPD, High Order Distortion

4 Conclusions

Even though the QPD spot becomes severely distorted, as modeled by Zemax, the X, Y position of the output spot centroid at the ETM transmission monitor QPD varies approximately linearly with the IFO beam displacement up to 4 mm at the ETM. This result holds true for up to 2.5 waves of combined astigmatic and comatic optical distortion, and up to 1.0 wave of high order distortion which would simulate distortion lumps in the optic of size 80 mm, in the central 160 mm clear aperture of the reaction mass.

The primary observable effect of optical distortion in the reaction mass is to offset the spot centroid by a constant amount along an axis determined by the azimuthal axis of the distortion. This constant offset can be eliminated in all cases by steering the beam centroid to the center of the QPD during initial alignment.

It appears that the ADLIGO ETM reaction mass can be specified to have less than 2.5 waves of phase irregularity in transmission over the central 160 mm diameter clear aperture of the optic.